# Stony Brook University

# Histomorphometric Differences in Tibial Cortical Bone Based on Sampling Location

A Thesis Presented

By

**Stephanie Nicole Blatch**

to

The Graduate School

in Partial Fulfillment of the Requirements

for the Degree of

**Master of Arts**

in

**Anthropology**

**(Physical Anthropology)**

Stony Brook University

**August 2012**

**Stony Brook University**

The Graduate School

**Stephanie Nicole Blatch**

We, the thesis committee for the above candidate for the

Master of Arts degree, hereby recommend

acceptance of this thesis.

**Dr. Frederick E. Grine – Thesis Advisor**
**Professor, Department of Anthropology**

**Dr. Karen L. Baab – Second Reader**
**Assistant Professor, Department of Anthropology**

**Dr. William L. Jungers – Outside Committee Member**
**Distinguished Teaching Professor and Chair, Department of Anatomical Sciences**

This thesis is accepted by the Graduate School

Charles Taber
Interim Dean of the Graduate School

Abstract of the Thesis

**Histomorphometric Differences in Tibial Cortical Bone Based on Sampling Location**

by

**Stephanie Nicole Blatch**

**Master of Arts**

in

**Anthropology**

**(Physical Anthropology)**

Stony Brook University

**2012**

Histomorphometric analysis of cortical bone is often used to estimate age at death of skeletons or to make inferences about mobility in past populations. Although previous studies have indicated that remodeling is variable within a single cross-section of bone, there has been little examination of the nature of these differences in the human tibia. This study investigated whether there are differences in remodeling based on sampling location in human tibiae, specifically examining inter-quadrant differences (anterior, posterior, medial, and lateral) as well as differences between periosteal, endosteal, and midcortical sampling locations.

Slides of undecalcified sections of human tibiae at midshaft (N=10) were used to analyze histomorphometric properties including percent remodeled bone, osteon population density (OPD), Haversian canal size, and osteon size.

Results indicate that there is a difference in remodeling of the cortical bone that is dependent on sampling location. Remodeling parameters differ between anatomical quadrants, with the anterior quadrant typically exhibiting higher rates of remodeling. Midcortical sampling locations exhibited greater remodeling than either endosteal or periosteal regions. Furthermore, the selection of magnification level and field size can significantly affect the measurement of OPD. These results support the idea that remodeling can progress in contrasting ways between various areas of the same cross-section of bone. Therefore, care should be taken when comparing histomorphometric properties from different areas of tibial cortical bone.

## Table of Contents

## List of Tables

## List of Figures

## INTRODUCTION

As do most tissues of the body, human bone undergoes a constant process of repair and replacement. The micro-morphology of bone is affected by its resorption and deposition through modeling as well as by replacement through remodeling. Bone remodeling is the process by which existing primary bone is resorbed and replaced by the deposition of newly formed secondary bone. The osteoclasts and osteoblasts that work together to accomplish this process comprise basic multicellular units (BMUs), which replace packets of primary bone with newer bone tissue (Martin and Burr, 1989). The result is the formation of secondary osteons, which, for simplicity's sake, are referred to here as osteons. Cooper et al. (1966) defined an osteon as "an irregular branching, and anastomosing cylinder composed of a more or less centrally placed, cell-containing, neurovascular canal, surrounded by concentric, cell-permeated lamellae of bone matrix." In cross section, osteons appear as areas where roughly-circular, concentric lamellae surround a central vascular channel, the Haversian canal, which typically measures 50 to 90 μm in diameter (Frost, 1961). The lamallae of each osteon are surrounded by a cement line, which indicates where the reversal from bone resorption to bone deposition took place (Martin and Burr, 1989).

Although the stimulus for and mechanism by which the BMUs are activated to remodel bone, as well as the degree to which such remodeling can be targeted are still being investigated, research indicates that remodeling functions to repair low-level damage in bone tissue (e.g. Burr et al., 1985; Martin and Burr, 1989; Mori and Burr, 1993; Burr, 2002). Osteons can replace areas with microfracture damage, while the cement lines that surround osteons may slow or limit the propagation of microfractures

already in existence (Burr et al, 1988; Martin and Burr 1989). Microdamage in bone tends to accumulate with both loading and aging (e.g. Burr et al., 1985; Mori and Burr, 1993; Schaffler et al, 1995; Bentolila et al., 1998; Martin, 2000; Robling et al., 2006). Therefore, over the course of an individual's life, cortical bone is expected to appear increasingly remodeled (i.e. possess a higher density of osteons that have replaced primary bone).

This understanding of cortical bone remodeling has informed the fields of physical anthropology and forensic science. It provides an important tool for estimating adult age-at-death in forensic, archeological, and pre-historical circumstances. Age-related changes in human cortical bone have long been recognized (Jowsey, 1960) and the utility of the temporal increase in the proportion of remodeled bone for estimating skeletal age has been well-explored. For nearly fifty years, researchers have used samples from present-day human populations to explore changes in cortical bone with increasing age and to develop predictive equations by which age-at-death can be estimated. These estimates have employed differences in a variety of micromorphological attributes including osteon number, osteon fragment number, osteon population density (OPD), osteon size, Haversian canal size, and the percent remodeled bone (e.g. Kerley, 1965; Ahlqvist and Damsten, 1969; Kerley and Ubelaker, 1978; Thompson, 1979; Ericksen, 1991; Stout and Paine, 1992; Thomas et al., 2000; Cho et al., 2002; Streeter, 2010). When tested on skeletons of known age, these predictive equations based on bone histology (especially when used in combination with dental histology) have generally produced age estimates that both have narrower ranges and are more accurate than age estimates based solely on gross skeletal

morphology (e.g. pubic symphysis, ectocranial sutures, etc.) and are particularly useful in individuals of advanced age (Ritz-Timme et al., 2000; Rösing et al., 2007; Franklin, 2010). The use of microstructural changes in cortical bone morphology for the purpose of age estimation has been investigated in several sites throughout the skeleton – most commonly in the limb bones, ribs, and mandible. The variety of viable sampling locations for this technique carries the distinct advantage of making it applicable to partial skeletons or even fragmentary bones, providing an especially valuable tool for bioarchaeological investigations relating to ontogenetic age. This tool has been applied to the study of cortical remodeling rates in both recent and ancient populations (Abbott et al., 1996; Pfeiffer, 1998; Mays, 2001; Streeter et al., 2001; Cho et al., 2006; Streeter et al., 2010) and also used to make inferences about activity patterns in past populations (Burr et al, 1990; Larsen, 1997; Pfeiffer et al., 2006).

As might be expected, many studies have reported finding increased osteon population density and percentage of remodeled area as well as smaller average osteon sizes with advancing age. However, these results are neither universal nor without contradiction (for a review see Robling and Stout, 2008). Differences among studies of cortical microstructure may, in part, be due to differences in the ways in which data were collected. Indeed, variation between studies in data collection techniques seems omnipresent, with no established and commonly adhered to standards for collection. Therefore, differences in results may be affected by 1) using different definitions of what constitutes a whole osteon versus an osteonal fragment, 2) taking measurements with different levels of magnification and/or using different field sizes for data collection, 3) sampling from different areas of a bone cross-section (i.e. medial vs.

anterior, etc.), and 4) sampling from different regions of the bone (periosteal vs. endosteal). The ways in which osteons and fragments are variably defined can affect how many of the osteons present are included in a study. Different studies have set different standards for what counts as a whole osteon, but most seem to employ some combination of the percent of the Haversian canal and the percent of the total area of the osteon visible in the field of interest. All else being equal, studies that require, for example, only ninety percent of the Haversian canal to be visible will include more osteons per unit area than does a study that only includes osteons with the entire Haversian canal visible. Similarly, the magnification and size of the field of interest affects which osteons are counted as whole or as fragments. As the size of the field increases so does the ratio of its area to perimeter. Therefore, a larger field will have a smaller percentage of osteons that are truncated at its edges. As a result, larger fields are expected to have a greater ratio of whole to fragmentary osteons than smaller fields in which many osteons near the perimeter will not have complete Haversian canals within the region of interest. Another factor that may play a significant role in the variation between results of histomorphometric analyses is choice of sampling site. Studies have used a wide variety of sampling sites from bones throughout the body to study histomorphometric properties, and those that have included more than one bone (e.g. Kerley, 1965; Thompson, 1979; Stout and Paine, 1992) have found differences in histomorphometric variables between bones and differences in their relative effectiveness in predicting age. In a study of the effects of sampling location, Pfeiffer et al. (1995) found variation in cortical microstructure between quadrants within femoral

cross-sections. This variability within a single bone was corroborated by Chan et al. (2007), who reported both intra- and intersection variability in the human femoral cortex.

In histomorphometric analysis, the femur is the most commonly used bone to estimate age and make inferences about activity patterns, but the reported variability between femoral quadrants suggests that studies sampling from different areas may produce results that are not necessarily comparable. The tibia is also commonly employed to estimate age, but little of this type of location-specific sampling analysis has been applied to the tibia (Drapeau and Streeter, 2006). Indeed, even though there has been more histomorphometric research on the femur, studies of collagen fiber orientation suggest that the loading of the tibia is more standardized between individuals than is loading in the femur (Corando et al, 1989; Goldman et al., 2003). If true, this would mean that the tibia is a more desirable sampling location for making inferences about age and activity patterns. The low inter-individual variability of microstructure implied by collagen fiber studies makes the tibia a prudent sampling location for populations with small sample sizes, which may be skewed by the influence of a few individual specimens. Additionally, the tibia may be particularly useful in archeological contexts because of its robusticity and associated high rate of preservation in comparison with more gracile bones.

A better understanding of remodeling differences in the tibia will also be useful in the study of the distal lower limb bones as a functional complex. While the tibia plays the major role in weight-bearing, the fibula also has a weight-bearing function, transmitting approximately 6-19% of body weight (Lambert, 1971; Takehe et al., 1984; Goh et al., 1992; Wang et al., 1996; Funk et al., 2004). Furthermore, studies on athletes

have indicated that the cross-sectional geometric properties of both the tibia (Shaw and Stock, 2009; Nikander et al., 2010; Rantalainen et al., 2011) and fibula (Rantalainen et al., 2010, Marchi and Shaw, 2011) are responsive to loading. As such, both elements may be informative about locomotor behavior in past populations. The tibia and fibula exhibit differential responses to loading regimes on a macroscopic level (Rantalainen et al., 2010, Marchi and Shaw, 2011), which begs the question of how such loading regimes affect remodeling on a microscopic level. Examining the two bones of the leg will allow direct comparison of a loaded bone (the tibia) with a far less loaded bone (the fibula). This would appear to be a more apt comparison in evaluating the effects of loading than comparison of skeletal elements such as the femur and rib, which have been employed previously (Pfeiffer, 1998; Robling, 1998; Mulhern, 2000; Pfeiffer et al., 2006). The tibia and fibula share similar environments of local influences and load repetition but are differentially loaded and may better represent the effects of loading rates on cortical remodeling and diaphyseal robustiticy. A better understanding of cortical remodeling in the tibia will inform future comparative studies of microstructural variation within the tibia and the fibula.

Histomorphometric analysis of the tibia may also be of value in answering different questions than are posed in examination of the femur. Due to the fact that distal limb segments are more energetically costly to move (Alexander, 1998; Hildebrand and Goslow, 2001; Dellanini et al., 2003), the addition of extra weight through the deposition of more bone comes at a greater energetic cost in the tibia than in the femur. The tibia may therefore be under different constraints than the femur due to the competing pressures of maintaining sufficient bone strength while preserving

energetic efficiency of locomotion. There may therefore be a stronger relationship between the effects of mechanical loading and bone remodeling in the tibia than there is in the more proximal segments where extra bone is less costly. Lieberman and Crompton (1998) proposed that while proximal limb bones can adapt to high-strain loading regimes by simply increasing the cross-sectional area of their cortical bone, distal limb segments, where bone is more energetically costly, should instead exhibit more remodeling in response to greater microfracture and fatigue damage. It should be noted, however, that Stock (2006) actually found the opposite to be true at least in terms of diaphyseal shape and robusticity. He found that the proximal limb bones (humerus and femur) had lower variation in the estimates of their polar section moduli ($Zp \approx J^{0.73}$), which are indicators of diaphyseal torsional and bending strength, when compared with distal limb bones (ulna and tibia). Stock argued that the lower variation in proximal limb bones is evidence that these locations are examples of greater "optimization of form in relation to functional constraints, with minimal random or residual variation." Lieberman and Crompton's hypothesis also was not supported by the work of Drapeau and Streeter (2006) who investigated the comparative remodeling of the femur and tibia at midshaft. With regard to both cross-sectional geometry and histomorphometry, this study indicated that the tibia does not remodel more than the femur in response to loading. Interestingly, this study also reported non-uniform remodeling within a single cross-section indicating differential loading histories and/or responses to loading within the tibial cortex.

The present study comprises a detailed analysis of regional differences in remodeling within a cross-section of the human tibia. Specifically, this study will address

the questions of 1) how cortical remodeling in the tibia varies between quadrants of the same cross section, 2) how cortical remodeling in the tibia varies between the endosteal, periosteal, and midcortical regions of the bone, and 3) how the degree of magnification and the size of field of interest affect relevant measurements of cortical bone remodeling. In addition to providing a characterization of regional differences in tibial cortical remodeling, the results of this study will be informative regarding the comparability of various histomorphometric analyses of the tibia and will be informative for tibial sampling site selection in future histomorphometric investigation.

## METHODS AND MATERIALS

### The Sample

The bone samples for this study consist of slides of undecalcified sections of human tibiae from each of ten individuals taken from the forensic collection of the University of Missouri-Columbia. The sample consists of three female and seven male specimens with estimated ages based on gross skeletal morphology that range from 20-70+ years at time of death (see Table 1 and Figure 1). Tibial sections were taken at midshaft and prepared following routine histological procedures (see Drapeau and Streeter, 2006).

### Data Collection Tools and Techniques

Images were captured using an AxioCam MRc camera coupled to a Zeiss Axioskop 2 binocular compound microscope. Measurements were taken using Zeiss Axiovision software 4.4.1.0.

Images were captured at 100x magnification with each image measuring 0.670 mm by 0.897 mm, which resulted in fields of interest measuring approximately 0.601 $mm^2$. Consecutive images of cortical bone were taken in a single column from the endosteal surface to the periosteal surface of the tibia in four anatomical quadrants: anterior, posterior, medial, and lateral (Fig 2). The number of images within each column was variable (5 – 22 images per column) depending on the cortical thickness in each quadrant. Histomorphometric variables measured within each image included osteon count, fragment count, Haversian canal areas, osteon areas, and total remodeled area and were taken using semi-automated functions of Zeiss Axiovision 4.4.1.0. For a description of these variables, please see Table 2. To be considered a whole osteon, 90% of the Haversian canal had to be visible in the field of view. Osteons with less than 90% of the Haversian canal visible were counted as fragmentary osteons (Fig.3).

**Evaluation of Endosteal, Midcortical, and Periosteal Differences**

*Selection of images.* The endosteal and periosteal aspects of the tibiae were typically covered with layers of lamellar bone that appeared to sustain lower levels of remodeling than the bulk of the interior tibial cortex. These relatively unremodeled perimeters of lamellar bone extended approximately 0.5-1.0 mm from the periosteal and endosteal surfaces. To evaluate the significance of the differences in remodeling, histomorphometric measurements from the periosteal-most image and endosteal-most image were compared with those from an image taken from the center of the tibial cortex for each quadrant across all slides (Fig. 4).

*Statistical analysis.* Periosteal, endosteal, and mid-cortex values for OPD, osteon size, Haversian canal size, and percent remodeled area were compared for each quadrant using repeated measures ANOVAs of raw and rank-transformed data. Post-hoc pairwise comparisons with a Bonferroni correction were used to evaluate differences between sampling locations.

**Comparing Quadrants Using Endosteal to Periosteal Column of Cortex**

*Selection of images:* To ascertain the overall effect of sampling location within a tibial cross section on remodeling characteristics, all images from the entire endosteal to periosteal column of cortex in each anatomical quadrant were considered in this comparison between quadrants.

*Statistical analysis.* Comparisons of osteon population density (OPD), osteon size, Haversian canal size, and percent remodeled bone between quadrants were carried out within each slide using ANOVAs of both raw and rank-transformed data. Applying usual parametric procedures to rank-transformed data has been shown to increase robusticity to violations of normality by employing distribution-free statistical tests (non-parametric) while preserving statistical power (Conover and Iman, 1981). ANOVAs were coupled with robust post-hoc tests for multiple comparisons (Games-Howell) after discovering differences in the ANOVAs. Patterns across slides were evaluated using sign tests. Additionally, average osteon population density (OPD), average osteon size, average Haversian canal size, and average percent remodeled bone were compared between quadrants across all ten slides using repeated measures

ANOVAs for raw and rank-transformed data coupled with post-hoc pairwise comparisons using a Bonferroni correction.

### Comparing Quadrants Using Only Interior Cortex

*Selection of comparison images.* To see if the comparison between quadrants remained constant with the exclusion of the endosteal and periosteal lamellar bone, all statistical analyses for the comparison between quadrants were repeated using three consecutive images from the midpoint of the cortical bone in each quadrant (Fig 5).

*Statistical Analysis.* Osteon area, Haverisan canal area, OPD, and percent remodeled area were compared within each slide using ANOVAs of raw and rank-transformed data coupled with post-hoc pairwise comparisons between quadrants (Games-Howell) and sign tests. Comparisons between slides for mean values of these measurements were carried out with repeated measures ANOVAs of raw and rank-transformed data using pairwise post-hoc tests with a Bonferroni correction.

### Comparing Levels of Magnification/Field Size

*Data collection.* For each slide, two images – one at 40x magnification and one at 100x magnification – were taken from the same area of the anterior cortex of the tibia (Fig. 6). As discussed above, magnification at 100x resulted in images measuring 0.670 mm by 0.897 mm with area of approximately 0.601 $mm^2$ while 40x magnification resulted in images measuring 1.674 mm by 2.237 mm with an area of approximately 3.745 $mm^2$.

*Statistical Analysis.* Osteon area, Haversian canal area, OPD, and percent remodeled area were compared between 40x and 100x magnifications across all 10 slides using paired t-tests with both raw and rank-transformed data.

## RESULTS

### Evaluation of Endosteal, Midcortical, and Periosteal Differences

Histomorphometric variables were not uniform throughout the thickness of the cortical bone. A repeated measures ANOVA comparing endosteal and periosteal regions with the midpoint of the cortical thickness found mean osteon area to differ significantly by sampling location in all four quadrants (Figure 7), with the periosteal region generally containing smaller osteons than the midpoint and endosteal regions. However, mean Haversian canal area differed significantly between sampling locations only in the posterior quadrant with the endosteal region exhibiting larger canals than the periosteal region (Figure 8). Both OPD (Figure 9) and percent remodeled bone (Figure 10) differed significantly between sampling locations in all four quadrants of the cortex, with the midpoint of the cortex generally displaying signs of greater remodeling, including a greater density of osteons and fragments as well as a higher percent of remodeled area than the endosteal and periosteal regions. Table 3 contains a full report of comparisons between the endosteal, midpoint, and periosteal sampling locations.

Using rank-transformed data to explore differences in remodeling between the endosteal, periosteal, and interior cortical bone produced similar results. Differences in mean osteon area between sampling locations remained significant in all four anatomical quadrants with mean osteon size of the periosteal surface generally being

smaller than that of other sampling locations. Haversian canal size differed significantly between sampling locations for both the anterior and posterior quadrants, while differences in OPD and percent remodeled bone remained significant in all four quadrants (see Table 4 for test statistics and pairwise comparisons).

### Comparing Quadrants Using Endosteal to Periosteal Column of Cortex

*Within-slide comparisons*. Comparisons between quadrants within each slide indicated significant differences in osteon areas between quadrants in five of the ten slides (Table 5). Sign tests comparing quadrants indicated that larger osteon areas occur more frequently in the posterior quadrant compared to the medial ($p = 0.022$) and lateral ($p = 0.022$) quadrants than would be expected by chance. Six out of ten slides displayed significant differences in Haversian canal area between quadrants (Table 6), with a sign test showing larger Haversian canals in the anterior quadrant than the lateral quadrant ($p = 0.022$). Robust ANOVAs found differences in OPD in three out of ten slides (Table 7), while sign tests indicated that OPD is greater in the anterior quadrant than the posterior ($p = 0.002$), medial ($p = 0.002$), and lateral ($p = 0.022$) quadrants more often than expected by chance. Similarly, the percent of remodeled cortical area is more often greater in the anterior quadrant than the posterior ($p = 0.002$), medial ($p = 0.022$), and lateral ($p = 0.022$) quadrants, with significant differences occurring in six out of the ten slides examined (Table 8).

A within slide comparison of quadrants using rank-transformed data corroborates the general patterns of remodeling observed with the raw data. Six out of ten slides displayed significant differences in osteon areas between quadrants (Table 9), while a

sign test showed that the posterior quadrant contains larger osteons than the medial quadrant ($p = 0.022$). Differences in Haversian canal size were significant in seven slides (Table 10), with larger canals occurring more often in the anterior than the medial ($p = 0.022$) and lateral ($p = 0.022$) quadrants, and more often in the posterior than the lateral quadrant ($p = 0.022$). With ranked data, five out of ten slides displayed significant differences between quadrants in OPD (Table 11). The density of osteons and osteon fragments is more often greater in the anterior than the posterior quadrant ($p = 0.002$) and greater in the medial than the posterior quadrant ($p = 0.022$). Seven out of ten slides exhibited differences in the percentage of remodeled bone between quadrants (Table 12), with sign tests indicating that the anterior quadrant is significantly more remodeled than the posterior ($p = 0.002$), medial ($p = 0.022$), and lateral ($p = 0.022$) areas of the cortex.

*Between-slides comparison.* All four variables explored (average osteon area, Haversian canal area, OPD, and percent remodeled bone) differed significantly among quadrants. A repeated measures ANOVA ($F = 3.510$, $p = 0.029$) indicated that average osteon area is variable between areas of a cross-section. Post-hoc tests using a Bonferroni correction revealed that the posterior quadrant contains significantly larger osteons than the lateral quadrant (Fig. 11). A test of Haversian canal areas also indicated significant differences between sampling locations ($F = 5.985$, $p = 0.003$). However, the post-hoc pairwise comparisons failed to reach statistical significance. The lack of significant pairwise tests may also be partially driven by one extreme outlier of a particularly large Haversian canal in the lateral quadrant (Fig. 12). Average OPD differed between quadrants ($F = 12.042$, $p < 0.001$). Post-hoc tests revealed that OPD

can be distinguished between the anterior and posterior ($p < 0.001$) and anterior and medial ($p = 0.004$) cortices with the anterior cortex exhibiting significantly higher levels of remodeling (Fig. 13). A repeated measures ANOVA indicated highly significant differences in the average percent of bone that is remodeled between areas in a cross-section ($F = 12.919$, $p < 0.001$), with the anterior cortex exhibiting significantly more remodeling than the posterior ($p=0.003$), medial ($p=0.016$), and lateral ($p=0.006$) cortices (Fig.14)

The aforementioned tests, when repeated with rank-transformed data, produced similar results. Average osteon area continued to differ between areas of the cortex ($F = 3.522$, $p = 0.028$), with the posterior quadrant containing larger osteons than the lateral quadrant ($p = 0.021$). There were significant differences between quadrants for Haversian canal areas ($F = 9.976$, $p < 0.001$), with the anterior quadrant sustaining larger Haversian canals than the medial ($p = 0.031$) and lateral ($p = 0.011$) quadrants. OPD differed significantly between quadrants ($F = 11.096$, $p < 0.001$), with osteon population being significantly denser in the anterior than the posterior ($p = 0.001$) and medial ($p = 0.002$) quadrants. The percent of remodeled bone also differed between quadrants ($F = 12.286$, $p < 0.001$). The anterior cortex had significantly greater area of remodeling than the posterior ($p = 0.003$), medial ($p = 0.025$), and lateral ($p = 0.005$) areas of the cortex.

### Comparing Quadrants Using Only Interior Cortex

*Within slide comparisons.* Using a sub-sample from the midpoint of the interior cortical bone only, as opposed to employing the entire endosteal to periosteal column of

cortex, reveals similar patterns of cortical remodeling. Three out of ten slides displayed significant differences in osteon size between quadrants (Table 13). Sign tests indicated that osteons are larger in the posterior than in the lateral quadrant ($p = 0.022$). Haversian canal size differed between quadrants in six of ten slides (Table 14), with the anterior cortex containing larger canals than the lateral cortex ($p = 0.022$). Three slides exhibited significant differences in OPD between quadrants (Table 15). Sign test indicated that both the anterior ($p = 0.002$) and medial ($p = 0.004$) quadrants have a consistently greater density of osteons and fragments than the posterior quadrant. The percent of remodeled bone differed between quadrants in three of the ten slides (Table 16) with the anterior quadrant consistently sustaining higher levels of remodeling than the posterior quadrant ($p = 0.002$).

The evaluation of inter-quadrant differences using rank-transformed data produced results that are extremely similar to the raw data from the interior cortex. Three of ten slides exhibited significant differences in osteon size between areas of the cortex (Table 17) while a sign test again showed osteon areas are consistently larger in the posterior quadrant compared with the lateral quadrant ($p = 0.022$). Significant differences in Haversian canal area were present in four out of ten slides (Table 18), with the anterior quadrant containing larger canals than the lateral quadrant ($p = 0.022$). The robust ANOVAs of ranked data from three slides indicated differences in OPD between quadrants (Table 19), with greater osteon densities in the anterior ($p = 0.002$) and medial ($p = 0.002$) quadrants than in the posterior quadrant. The percent of remodeled bone differed significantly between the quadrants in five of the ten slides

(Table 20) with the anterior quadrant displaying more remodeling than the posterior quadrant ($p = 0.039$).

*Between slides comparison.* In the comparison across all slides, differences in osteon areas between quadrants just reached significance ($F = 2.970$, $p = 0.050$) (Figure 15). Post-hoc comparisons indicated that osteon size is greater in the posterior than the lateral quadrant ($p = 0.047$). A repeated measures ANOVA for Haversian canal area revealed significant differences between quadrants ($F = 4.563$, $p = 0.010$), but as with the comparisons of the whole cortex, the conservative Bonferroni correction prevented post-hoc pairwise comparisons from reaching levels of significance (Figure 16). Differences in OPD between quadrants were found ($F = 8.278$, $p < 0.001$), with OPD being lower in the posterior quadrant than the anterior ($p = 0.002$) and medial ($p = 0.028$) quadrants (Figure 17). A repeated measures ANOVA for average percent of remodeled bone also revealed significant differences between quadrants ($F = 3.361$, $p = 0.033$), with the anterior tibial cortex showing significantly more remodeling than the posterior cortex ($p = 0.016$) (Figure 18).

An examination of ranked data produced similar results. Haversian canal size remained significantly different between quadrants ($F = 7.983$, $p = 0.001$), with the anterior quadrant containing larger Haversian canals than the lateral quadrant ($p = 0.022$). A repeated measures ANOVA with ranked data indicates no differences in osteon area between quadrants ($F = 1.303$, $p = 0.294$). With ranked data, OPD continues to differ significantly between areas of the cortex ($F = 6.703$, $p = 0.002$), with the posterior quadrant containing a lower density of osteons than the anterior ($p = 0.003$) and medial ($p = 0.037$) quadrants. A repeated measures ANOVA for ranked data

of percent remodeled area also indicates differences between quadrants ($F = 3.004$, $p = 0.048$). However, the post-hoc pairwise comparisons failed to reach statistical significance.

### Comparing Levels of Magnification/Field Size

Using raw and rank-transformed data to compare histomorphometric variables between 40x and 100x images produced essentially identical results. The variable most affected by magnification level and field size was OPD. The paired t-tests of raw and ranked data indicated significant differences in OPD between 40x and 100x images (raw: $t = -4.100$, $p = 0.003$; ranked: $t = -3.597$, $p = 0.006$), with 100x images containing higher densities of whole and fragmentary osteons (Figure 19). For both raw and rank-transformed data, there were no significant differences in osteon area, Haversian canal area, or percent remodeled bone between magnification levels (see Table 21, Figures 20-22).

### Age Correlations

Spearman's rank correlations did not indicate relationships between any of the four histomorphometric variables and age using either the entire column of cortex (Table 22) or only the interior cortex (Table 23).

## DISCUSSION

### Differences Between Histomorphometric Parameters Based on Sampling Location

Histomorphometric variables are not uniform throughout the thickness of the cortical bone. Cortical remodeling parameters differ between endosteal, periosteal, and mid-cortical sampling locations in all four quadrants. This means that choice of sampling location within the cortex has profound effects for age estimation and quantification of histomorphometric properties, regardless of the anatomical area of the cross-section chosen for sampling. The strongest signal that was observed is that the mid-cortex sustained consistently higher levels of remodeling, with elevated OPD and percent of remodeled bone, compared with the endosteal and periosteal regions. This result is unsurprising due to the fact that the endosteal and particularly the periosteal surfaces were often ringed by layers of lamellar bone, which appeared generally less remodeled than the interior of the cortical thickness. The variation in histomorphometric variables between sampling locations within the breadth of the cortex agrees with a similar exploration of variation in the human femur (Pfeiffer et al., 1995) whose rates of remodeling in the periosteal regions were generally depressed compared with those of sampling areas further toward the center of the cortical thickness. Unfortunately, Pfeiffer et al. (1995) did not extend the sampling for their study to the endosteal surface of the femur, so a comparison between all three femoral sampling locations (endosteal, midpoint, and periosteal) was not possible. Nevertheless, the similarity between the tibia and femur in remodeling through the cortex suggests that higher levels of mid-cortical remodeling may be common to cross-sections of all long bones. This difference should be considered when choosing or comparing sampling sites. The differences in remodeling parameters dependent on sampling location suggest that studies that have sampled exclusively from regions adjacent to the periosteal or endosteal surfaces may

represent the remodeling process differently than studies that have taken samples through the entire thickness of the tibial cortex.

The results of this study also indicate that remodeling does not take place uniformly between the different anatomical regions of the human tibia at midshaft. The four histomorphometric parameters that were measured here differed significantly by sampling location. Generally, within-slide and between-slides analyses agreed on the nature of these differences. The most striking and recurrent dissimilarities indicate that the anterior quadrant differs from the rest of the tibial cortex in the overall amount of remodeling it sustains. Previously, Drapeau and Streeter (2006) found remodeling in the tibial midshaft to be greater in the A-P axis than the M-L axis of the bone. From the results of this study, it now appears that the greater remodeling of the A-P axis is, in fact, driven by differences in the anterior quadrant. Both within and between slides, the anterior cortex contained higher OPD and a greater percent of remodeled bone as well as larger average Haversian canal size. Together, these findings suggest that the anterior cortical bone in the tibia at midshaft remodels at a faster rate than the other three quadrants of the cortex. The results of this study indicate that tibial sampling location can have a profound effect on the development of regression equations that can be used to predict age from histomorphometric variables. Therefore, results from studies that have sampled from the medial or lateral cortices of the tibia (Thompson and Galvin, 1983) or that have employed samples from multiple locations within the tibial cortex (Kerley, 1965; Uytterschaut 1985, 1993) may not be comparable with the results of studies that sampled only the anterior area of the tibia (Balthazard and Lebrun, 1911; Singh and Gunberg, 1970; Hauser et al., 1980).

The results of this study contrast with those of Pfeiffer et al. (1995) on human femoral cross-sections, where they reported that the anterior cortex of the femur exhibited a lower mean level of remodeling than other quadrants. Evidently, patterns of remodeling do not necessarily correlate between these two bones according to anatomically defined axes. The factors that influence such differential rates of remodeling remain unclear. However, variable loading between tibial quadrants is a likely influence. Studies on humans (Kimura, 1974; Peterman et al., 2001) and other primates (Demes et al., 2001) indicate that tibial loading primarily consists of bending forces with maximum strain in an A-P orientation. It is possible that remodeling responds strongly to the A-P bending forces of locomotion, particularly the tensile loading placed primarily on the anterior cortex. Future research should focus on possible influences for such regional differences within cross-sections such as variable loading regimes, the effect of load sharing between the tibia and fibula, and influences of muscular attachment sites.

In this study, a reevaluation of inter-quadrant differences using only interior cortical sampling locations produced the same general patterns of differences between quadrants as did comparisons using the full endosteal-periosteal columns of bone. There is, however, decreased signal when only the interior sampling location is used. It appears that the amount of unremodeled lamellar bone that surrounds each quadrant plays a partial role in driving inter-quadrant differences within a single cross-section. However, significant inter-quadrant differences still remain when comparing only interior sampling locations, which indicates there are still other factors, such as possibly differential loading regimes, at play in influencing regional differences in remodeling.

With regard to the use of cortical remodeling for age estimation, sub-periosteal sampling is commonly employed in the tibia as well as other long bones, particularly the femur (Kerley, 1965; Ahlqvist and Damsten, 1969; Singh and Gunberg, 1970; Thompson, 1979; Fangwu, 1983; Thompson and Galvin, 1983; Uytterschaut 1985; Cera and Drusini, 1985; Drusini, 1987; Narasaki, 1990; Ericksen, 1991, Uytterschaut 1993). However, researchers should be aware that studies sampling from sub-periosteal areas only may not be comparable with studies that sample from a variety of locations throughout the cortical thickness (Balthazard and Lebrun, 1911; Hauser et al., 1980; Samson and Branigan, 1987; Watanabe, 1998). Sub-periosteal sampling may be useful in age estimation because sub-periosteal areas area generally less remodeled than more interiorly located cortex. The faster remodeling of the interior cortex may cause the midcortical region to become saturated with osteons at an earlier age, which limits the ability to distinguish younger individuals from older individuals. The unremodeled lamellar bone along the periosteal surface may allow for a more fine-grained analysis of age-related changes as it remodels at a slower rate. On the other hand, examining remodeling of the periosteal lamellar bone may provide the muddled signals of modeling in addition to remodeling as more lamellar bone is laid down. Such sampling sites may therefore not be suitable for studies that wish to investigate remodeling responses to microdamage or activity, where increased bone thickness through modeling is likely. It is possible that sub-periosteal sampling may provide for finer grained age estimates, but such sampling should be undertaken with the understanding that samples from the periosteal region are not necessarily indicative of the rates of cortical remodeling taking place in the interior (or endosteal) cortex. Because the vast majority of cortical area is

neither adjacent to the periosteal nor endosteal surfaces, mid-cortical sampling is more representative of remodeling processes present in the majority of the cortical area within a cross section. In future studies, sampling site(s) throughout cortical breadth should be selected carefully to best address specific questions posed with regard to remodeling in cortical bone.

## Effects of Magnification Level and Field Size on the Measurement of Remodeling Parameters

As expected, the level of magnification and resultant field size did not have a significant effect on average osteon area, average Haversian canal area, or the overall percent of remodeled bone. However, the measurement of OPD was significantly affected by the size of the field under investigation. The variation in OPD between 40x and 100x magnification is a product of the ways in which osteons and osteon fragments are defined. Osteons that were partially cut off by the edges of the field of view were included in the category of osteon fragments. An image recorded at 100x magnification produces a smaller field of view than an image at 40x magnification. The greater ratio of perimeter to area of the smaller field results in more osteons at the edges of each image, and a consequential inflation in the count of osteonal fragments. Despite the inflation of OPD in smaller fields of view, the advantage of greater magnification is the detail with which cortical morphology can be distinguished. The advantage of being able to properly distinguish remodeled from unremodeled area and the surety with which cement lines can be located at a higher magnification outweighs the disadvantages of inflating the measurement of OPD. However, to correct for the issue of OPD inflation,

field size may be increased by digitally stitching together consecutive images, or a more universal system for determining what should be included or excluded from the category of osteon fragments could be developed. One suggestion would be to base the definition for a whole osteon on the presence of a complete Haversian canal (100 percent) without regard to the percent of osteonal lamellar bone included in the field of view. Osteons partially obscured by the edges of the field could be included in measurements on an alternate basis. Additionally, the shape of Haversian canals should be a criterion in the inclusion (and exclusion) of osteons from measurement. Osteons with Haversian canals that have a maximum width that is more than twice their maximum height should be excluded from analysis to avoid the inflation of osteon and Haversian canal areas that results from failing to transect an osteon perpendicular to its direction of propagation. Due to the fact that OPD, whole osteon counts, and osteon fragment counts are common parameters in the evaluation of age estimation (e.g. Kerley, 1965; Singh and Gunberg, 1970; Thompson, 1979; Hauser et al., 1980; Fangwu, 1983; Ericksen, 1991; Kimura, 1992; Stout and Paine, 1992; Stout et al., 1994; Stout et al., 1996, Cho et al., 2002; Cho et al., 2006), any comparisons between studies with different methodologies for data collection should carefully consider the sizes of the fields analyzed, and the criteria that have been employed in counting osteons and osteon fragments to ensure that the data are, indeed, comparable.

### Age-related Correlations of Remodeling Parameters

It has long been recognized that there are age-related changes in the morphology and properties of human cortical bone, which make age estimation based

on cortical micro-morphology possible (e.g. Jowsey, 1960; Wall et al., 1979; McCalden et al., 1993; Zioupos and Currey, 1998; Diab et al., 2006). However, this study did not find any significant correlations between age and the four remodeling parameters investigated (osteon area, Haversian canal area, OPD, percent remodeled bone). The lack of age correlations in this study is most likely due to the imprecise nature of the ages for the tibiae sampled, as well as the small sample size of individuals studied. In the future, an examination of inter-quadrant differences with a larger sample of known-age specimens would be necessary for the exploration of which remodeling parameters and quadrants most accurately predict the ontogenetic age of a skeleton.

## CONCLUSIONS

Although changes in human cortical bone can be useful both for understanding important biochemical and structural imperatives of bone replacement and for the estimation of age-at-death of skeletons, it is important to recognize that these changes are both complex and variable. The results of this study indicate that remodeling parameters in the tibia can vary between anatomical quadrants, and between areas sampled within the same quadrant dependent on distance from the endosteal and periosteal surfaces of the bone. Furthermore, the methods used for data collection can have a profound impact on measurement outcomes of histological variables. Magnification level and size of the field of view in conjunction with an individual researcher's decisions regarding the inclusion (or exclusion) of various components of remodeling morphology can create variability in measurement outcomes even within the same area of cortical bone. Further exploration of histomorphometric variability will lead

us to a deeper understanding of true cortical micro-morphology and the processes behind it, while greater standardization of research techniques will allow us to employ that understanding to develop the best possible age-determination methods using human cortical bone.

## REFERENCES


Abbott S, Trinkaus E, Burr DB. 1996. Dynamic bone remodeling in later Pleistocene fossil hominids. Am J Phys Anthropol 99:585-601.

Ahlqvist J, Damsten, O. 1969. A modification of Kerley's method for the microscopic determination of age in human bone. J Forensic Sci 14:205-212.

Alexander RM. 1998. Symmorphosis and safety factors. In: Weibel ER, Taylor CR, Bolis L, editors. Principles of animal design: the optimization and symmorphosis debate. Cambridge: Cambridge University Press. p 28-35.

Balthazard V, Lebrun L. 1911. Les canaux de Havers de l'os humain aux différents âges. Ann Hyg Publ Méd Lég. XV:144-152.

Bentolila V, Boyce TM, Fyhrie DP, Drumb R, Skerry TM, Schaffler MB. 1998. Intracortical remodeling in adult rat long bones after fatigue loading. Bone 23:275-281.

Burr DB. 2002. Targeted and nontargeted remodeling. Bone 30:2-4.

Burr DB, Martin RB, Schaffler MB, Radin EL. 1985. Bone remodeling in response to *in vivo* fatigue microdamage. Bone 18:189-200.

Burr DB, Schaffler MB, Frederickson RG. 1988. Composition of the cement line and its possible mechanical role as a local interface in human compact bone. J Biomech 11:939-945.

Burr DB, Ruff CB, Thompson DD. 1990. Patterns of skeletal histologic change through time: comparison of an archaic Native American population with modern populations. Anat Rec 226:307-313.

Cera F, Drusini A. 1985. Analisi critica e sperimentale dei metodi di determinazione dell'eta attraverso le microstrutture ossee. Quaderni di Anatomia Pratica XLI:105-121.

Chan AHW, Crowder CM, Rogers TL. 2007. Variation in cortical bone histology within the human femur and its impact on estimating age of death. Am J Phys Anthropol 132:80-88.

Cho H, Stout SD, Madsen RW, Streeter MA. 2002. Population-specific histological age-estimating method: a model for known African-American and European-American skeletal remains. J Forensic Sci 47:12-18.

Cho H, Stout SD, Bishop TA. 2006. Cortical bone remodeling rates in a sample of African American and European American descent groups from the American Midwest: comparisons of age and sex in ribs. Am J Phys Anthropol 130:214-226.

Conover WJ, Iman RL. 1981. Rank transformations as a bridge between parametric and nonparametric statistics. Am Stat 35:124-129.

Cooper RR, Milgram JW, Robinson RA. 1966. Morphology of the osteon. An electron microsopic study. J Bone Joint Surg 48A:1239-1271.

Corando S, Portigliatti Barbos M, Ascenzi A, Boyde A. 1989. Orientation of collagen in human tibial and fibular shaft and possible correlation with mechanical properties. Bone 10:139-142.

Dellanini L, Hawkins D, Martin RB, Stover S. 2003. An investigation of the interactions between lower-limb bone morphology, limb inertial properties and limb dynamics. J Biomech 36:913-919.

Demes B, Qin Y-X, Stern, JTJ, Larson SG, Rubin CT. 2001. Patterns of strain in the macaque tibia during functional activity. Am J Phys Anthropol 116:257-265.

Diab T, Condon KW, Burr DB, Vashishth D. 2006. Age-related change in the damage morphology of human cortical bone and its role in bone fragility. Bone 38:427-431.

Drapeau MSM, Streeter MA. 2006. Modeling and remodeling responses to normal loading in the human lower limb. Am J Phys Anthropol 129:403-409.

Ericksen MF. 1991. Histological estimation of age at death using the anterior cortex of the femur. Am J Phys Anthropol 84:171-179.

Fangwu Z. 1983. Preliminary study on determination of bone age by microscopic method. Acta Anthropol Sinica II:142-151.

Franklin D. 2010. Forensic age estimation in human skeletal remains: current concepts and future directions. Legal Med 12:1-7.

Frost HM. 1961. Human Haversian system measurements. Henry Ford Hosp Med Bull 9:145-147.

Funk JR, Rudd RW, Kerrigan JR, Crandall JR. 2004. The effect of tibial curvature and fibular loading on the tibia index. Traff Inj Prev 5:164-172.

Goh JCH, Lee HH, Ang EJ, Bayon P, Pho RWH. 1992. Biomechanical study on the load-bearing characteristics of the fibula and the effects of fibular resection. Clin Orthop 279:223-228.

Goldman HM, Bromage TB, Thomas, CDL, Clement JG. 2003. Preferred collagen fiber orientation in the human midshaft femur. Anat Rec [A] Discov Mol Cell Evol Biol 272:434-445.

Hauser R, Barres D, Durigon M, Derobert L. 1980. Identification par l'histomorphometrie du femur et du tibia. Acta Med Leg Soc 30:91-97.

Hildebrand M, Goslow GE Jr. 2001. Analysis of vertebrate structure. New York: John Wiley & Sons, Inc.

Jowsey J. 1960. Age changes in human bone. Clin Orthop Relat Res 17:210-218.

Kerley ER. 1965. The microscopic determination of age in human bone. Am J Phys Anthropol 23:149-64.

Kerley ER, Ubelaker DH. 1978. Revisions in the microscopic method of estimating age at death in human cortical bone. Am J Phys Anthropol 49:545-546.

Kimura T. 1974. Mechanical characteristics of human lower leg bones. J Faculty Sci Univ Tokyo Sect V Anthropol 4:319-398.

Kimura K. 1992. Estimation of age at death from second metacarpals. Z Morph Anthropol 79:169-181.

Lambert KL. 1971. The weight-bearing function of the fibula. J Bone Joint Surg 53A:507-513.

Larsen CS. 1997. Bioarchaeology: interpreting behavior from the human skeleton. Cambridge: Cambridge University Press.

Lieberman DE, Crompton AW. 1998. Responses of bone to stress: constraints on symmorphosis. In: Webel ER, Taylor CR, Bolis L, editors. Principles of animal design: the optimization and symmorphosis debate. Cambridge: Cambridge University Press. p 78-86.

Marchi D, Shaw CN. 2011. Variation in fibular robusticity reflects variation in mobility patterns. J Hum Ev 61:609-616.

Martin RB. 2000. Toward a unifying theory of bone remodeling. Bone 26:1-6.

Martin RB. 2007. Targeted bone remodeling involves BMU steering as well as activation. Bone 40:1574-1580.

Martin BR, Burr DB. 1989. Structure, function, and adaptation of compact bone. New York: Raven Press.

Mays S. 2001. Effects of age and occupation on cortical bone in a group of 18$^{th}$-19$^{th}$ century British men. Am J Phys Anthropol 116:34-44.

McCalden RW, McGeough JA, Barker MB, Court-Brown CM. 1993. Age-related

changes in the tensile properties of cortical bone. The relative importance of changes in porosity, mineralization, and microstructure. J Bone Joint Surg Am 75:1193-1205.

Mori S, Burr DB. 1993. Increased intracortical remodeling following fatigue damage. Bone 14:103-109.

Mulhern DM. 2000. Rib remodeling dynamics in a skeletal population from Kulubnarti, Nubia. Am J Phys Anthropol 111:519-530.

Narasaki S. 1990. Estimation of age at death by femoral osteon remodeling: application of Thompson's core technique to modern Japanese. J Anthropol Soc Nippon 98:29-38.

Nikander R, Kannus P, Rantalainen T, Uusi-rasi K, Heinonen A, Sievänen H. 2010. Cross-sectional geometry of weight-bearing tibia in female athletes subjected to different exercise loadings. Osteoporosis Int 21:1687-1694.

Peterman MM, Hamel AJ, Cavanagh PR, Piazza SJ, Sharkey NA. 2001. In vitro modeling of human tibial strains during exercise in micro-gravity. J Biomech 34:693-698.

Pfeiffer S, Lazenby R, Chiang J. 1995. Brief communication: cortical remodeling data are affected by sampling location. Am J Phys Anthropol 96:89-92.

Pfeiffer S. 1998. Variability in osteon size in recent human populations. Am J Phys Anthropl 106:219-227.

Pfeiffer S, Crowder C, Harrington L, Brown M. 2006. Secondary osteon and Haverisan canal dimensions as behavioral indicators. Am J Phys Anthropol 131:460-468.

Rantalainen T, Nikander R, Daly RM, Heinonen A, Suominen H, Sievänen H. 2010. Direction-specific diaphyseal geometry and mineral mass distribution of the tibia and fibula: a pQCT study of female athletes representing different exercise loading types. Calcif Tissue Int 86:447-454.

Rantalainen T, Nikander R, Daly RM, Heinonen A, Sievänen H. 2011. Exercise loading and cortical bone distribution at the tibial shaft. Bone 48:786-791.

Ritz-Timme S, Cattaneo C, Collins MJ, Waite ER, Schütz HW, Kaatsch HJ. 2000. Age estimation: the state of the art in relation to the specific demands of forensic practice. Int J Legal Med 113:129-136.

Robling AG. 1998. Histomorphometric assessment of mechanical loading history from human skeletal remains: the relationship between mircromorphology and macromorphology at the femoral midshaft. Ph.D. dissertation, University of Missouri-Columbia.

Robling AG, Castillo AB, Turner CH. 2006. Biomechanical and molecular regulation of bone remodeling. Annu Rev Biomed Eng 8:455-498.

Robling AB, Stout SD. 2008. Histomorphometry of human cortical bone: applications to age estimation. In: Katzenberg MA, Saunders SR, editors. Biological anthropology of the human skeleton. Hoboken: Wiley-Liss. p 149-182.

Rösing FW, Graw M, Marré B, Ritz-Timme S, Rothschild MA, Rötzscher K, Schmeling A, Schröder I, Geserick G. 2007. Recommendations for the forensic diagnosis of sex and age from skeletons. Homo 58:75-89.

Samson C, Branigan K. 1987. A new method of estimating age at death from fragmentary and weathered bone. In: Boddington A, Garland AN, Janaway RC, editors. Death decay and reconstruction approaches to archaeology and forensic science. Manchester: Manchester University Press. p 101-108.

Schaffler MB, Choi K, Milgrom C. 1995. Aging and matrix microdamage accumulation in human compact bone. Bone 17:521-525.

Shaw CN, Stock JT. 2009. Intensity, repetitiveness and directionality of habitual adolescent mobility patterns influence the tibial diaphysis morphology of athletes. Am J Phys Anthropol 140:149-159.

Singh IJ, Gunberg DL. 1970. Estimation of age at death in human males from quantitative histology of bone fragments. Am J Phys Anthropol 33:373-381.

Stout SD, Paine RR. 1992. Histological age estimation using rib and clavicle. Am J Phys Anthropol 87:111-115.

Stout SD, Dietze WH, Iscan MY, Loth SR. 1994. Estimation of age at death using cortical histomorphometry of the sternal end of the fourth rib. J Forensic Sci 39:778-784.

Stout SD, Porro MA, Perotti B. 1996. Brief communication: a test and correction of the clavicle method of Stout and Paine for histological age estimation of skeletal remains. Am J Phys Anthropol 100:139-142.

Streeter, M. 2010. A four-stage method of age at death estimation for use in the subadult rib cortex. J Forensic Sci 55:1019-1024.

Streeter M, Stout SD, Trinkaus E, Stringer CB, Roberts MB, Parfitt SA. 2001. Histomorphometric age assessment of the Boxgrove 1 tibial diaphysis. J Hum Evol 40:331-338.

Streeter M, Stout S, Trinkaus E, Burr D. 2010. Brief communication: Bone remodeling rates in Pleistocene humans are not slower than the rates observed in modern populations: a reexamination of Abbott et al. (1996). Am J Phys Anthropol 141:315-318.

Stock JT. 2006. Hunter-gatherer postcranial robusticity relative to patterns of mobility, climatic adaptation, and selection for tissue economy. Am J Phys Anthropol 131:194-204.

Takebe K, Nakagawa A, Minami H, Kanazawa H, Hirohata K. 1984. Role of the fibula in weight-bearing. Clin Orthop 184:289-292.

Thomas CDL, Stein MS, Feik A, Wark JD, Clement JG. 2000. Determination of age at death using combined morphology and histology of the femur. J Anat 196:462-471.

Thompson DD. 1979. The core technique in the determination of age at death in skeletons. J Forensic Sci 24:902-915.

Thompson DD, Galvin CA. 1983. Estimation of age at death by tibial osteon remodeling in an autopsy series. Forensic Sci Int 22:203-211.

Uytterschaut HT. 1985. Determination of skeletal age by histological methods. Z Morphol Anthropol 75:331-340.

Uytterschaut HT. 1993. Human bone remodeling and aging. In: Grupe G, Garland AN, editors. Histology of ancient human bone: methods and diagnosis. New York: Springer-Verlag. p 95-109.

Wall JC, Chatterji SK, Jeffrey JW. 1979. Age-related changes in the density and tensile strength of human femoral cortical bone. Calcif Tissue Int 27:105-108.

Wang Q, Whittle M, Cunningham J, Kenwright J. 1996. Fibula and its ligaments in load transmission and ankle joint stability. Clin Orthop 330:261-270.

Wantanabe Y, Konishi M, Shimada M, Ohara H, Iwamoto S. 1998. Estimation of age from the femur of Japanese cadavers. Forensic Sci Int 98:55-65.

Zioupos P, Currey JD. 1998. Changes in the stiffness, strength, and toughness of human cortical bone with age. Bone 22:57-66.

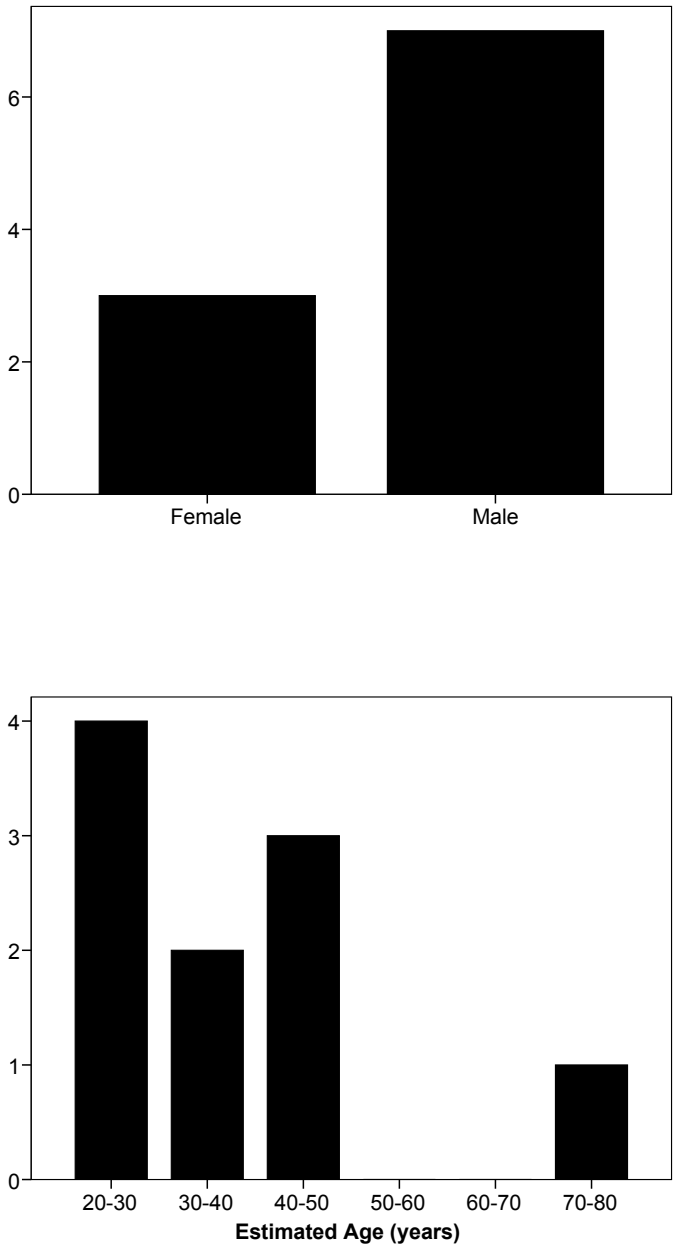


Figure 1. Age and sex frequency distributions for slides used in histological analysis (N = 10).

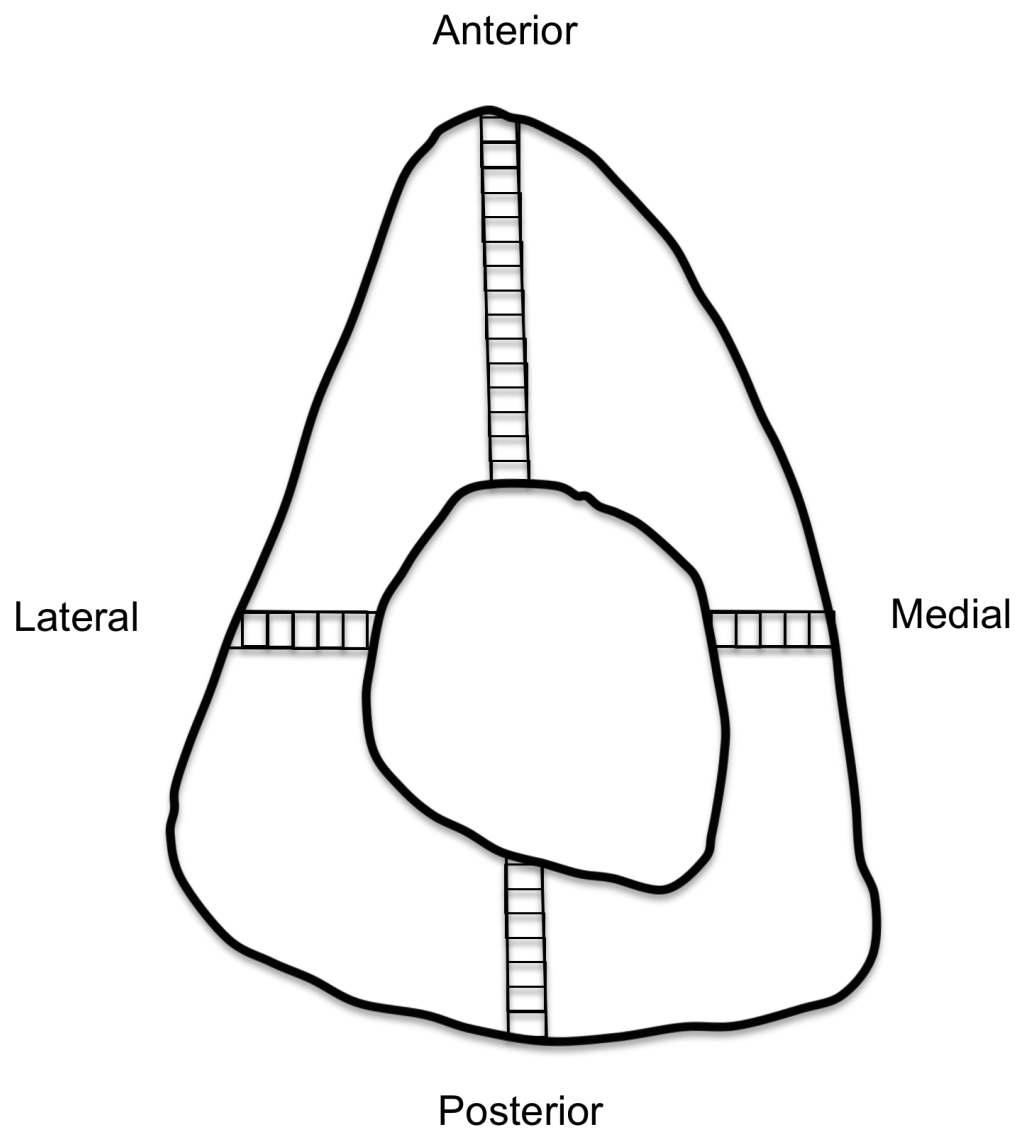


Figure 2. Image capture for data collection comparing remodeling parameters between anatomical quadrants of the tibia. Consecutive images of cortical bone were taken at 100x magnification in a single column from the endosteal surface to the periosteal surface in each of four quadrants (anterior, posterior, medial and lateral). The number of images per quadrant was variable and dependent on the thickness of the cortical bone in that quadrant. The above image illustrates an example in which 15 images were taken to cover the span of cortical bone through the anterior quadrant, 7 images through the posterior quadrant, 5 images through the lateral quadrant, and 5 images through the medial quadrant. Within each image, histomorphometric variables (osteon count, fragment count, osteon areas, Haversian canal areas, and total remodeled area) were measured using semi-automated functions of Zeiss Axiovision 4.4.1.0. Image not drawn to scale.

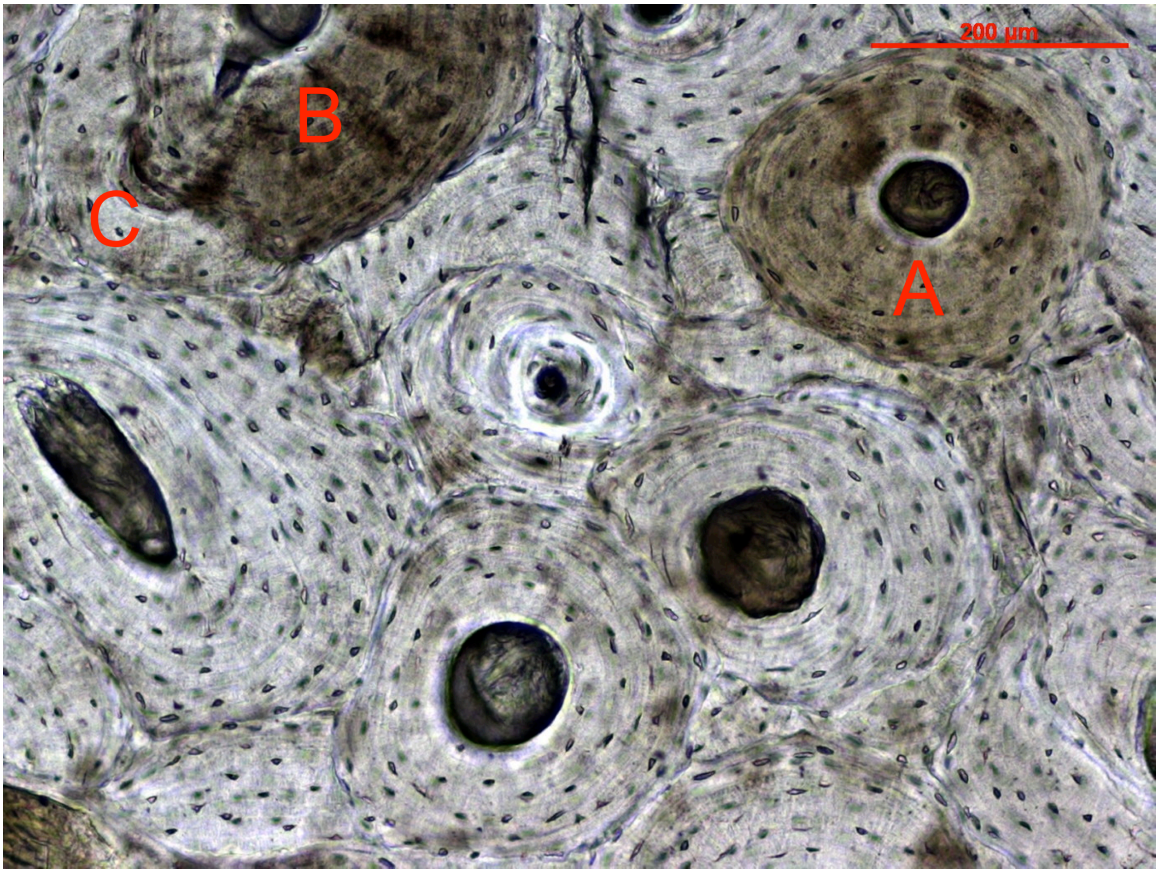


Figure 3. This field of interest exhibits several examples of whole osteons (such as “A”) and examples of what we considered to be osteon fragments. “B” was considered to be a fragment because its Haversian canal is not wholly within the field of view while “C” was also considered a fragment because its Haversian canal has been partially obscured by another osteon.

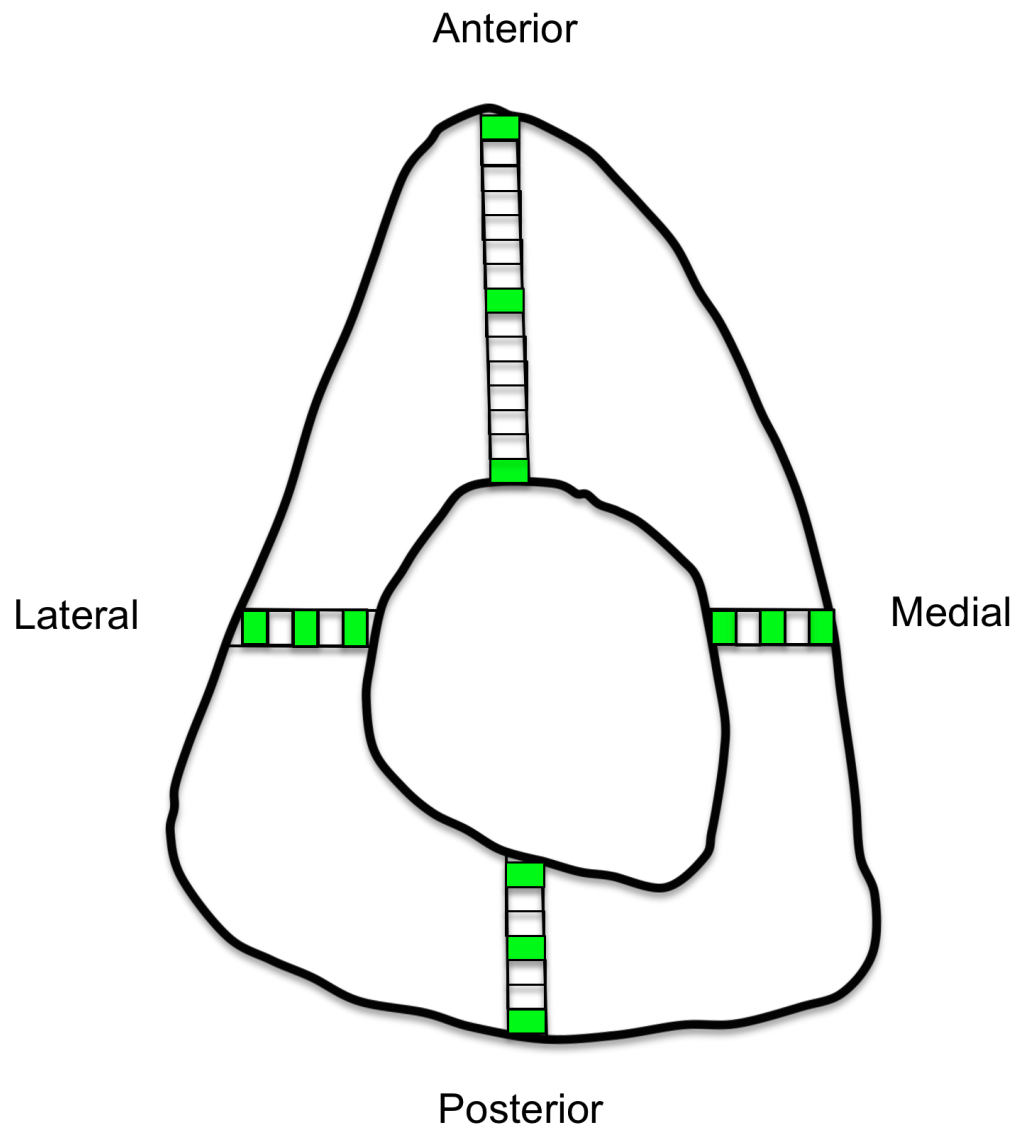


Figure 4. Image selection for comparison of endosteal, periosteal and mid-cortical remodeling. Histomorphometric parameters were compared between the endosteal-most, periosteal-most and midpoint images of each quadrant. Image not drawn to scale.

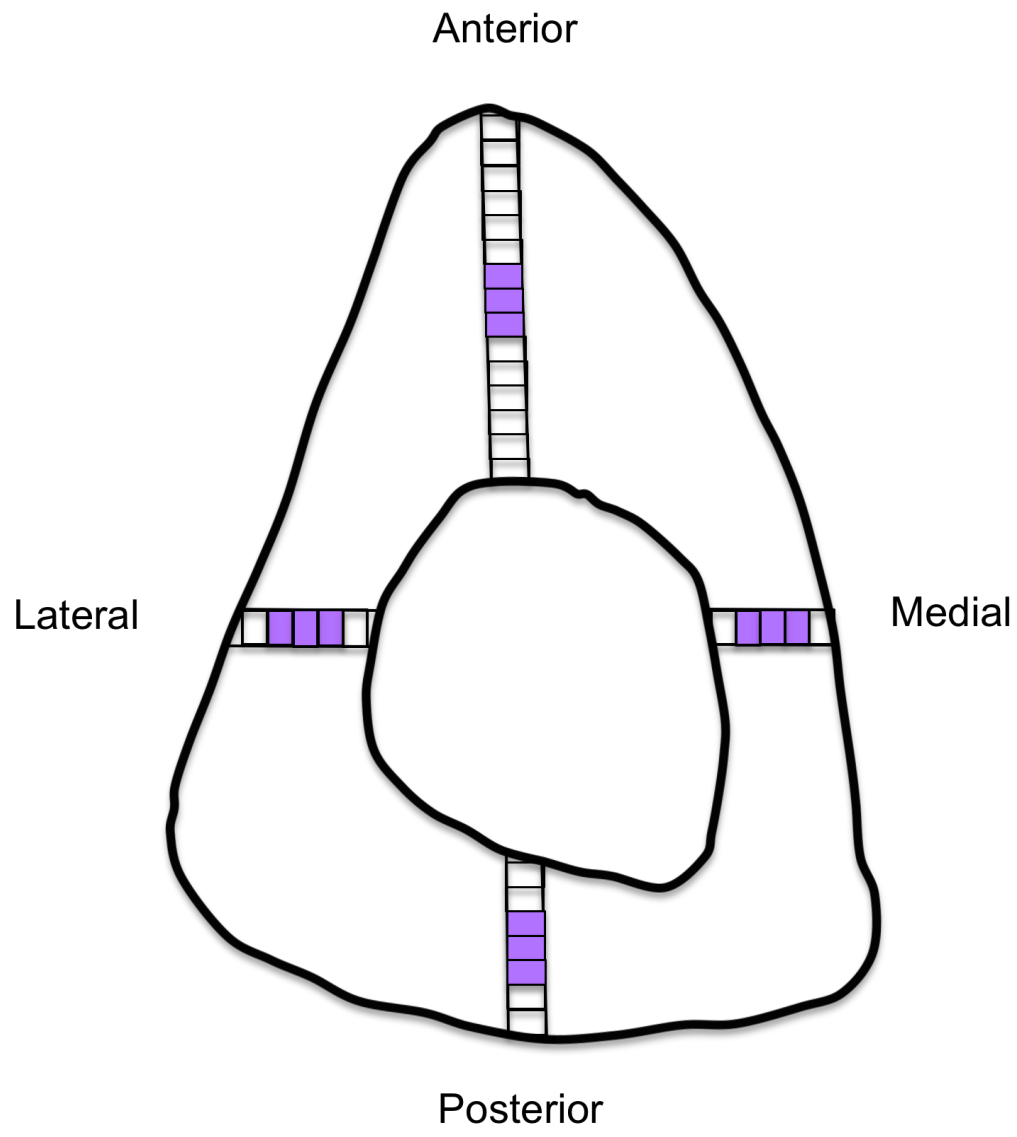


Figure 5. Image selection for comparing remodeling parameters between quadrants using interior cortex only. Three consecutive images surrounding the midpoint of each quadrant were selected for analysis. Image not drawn to scale.

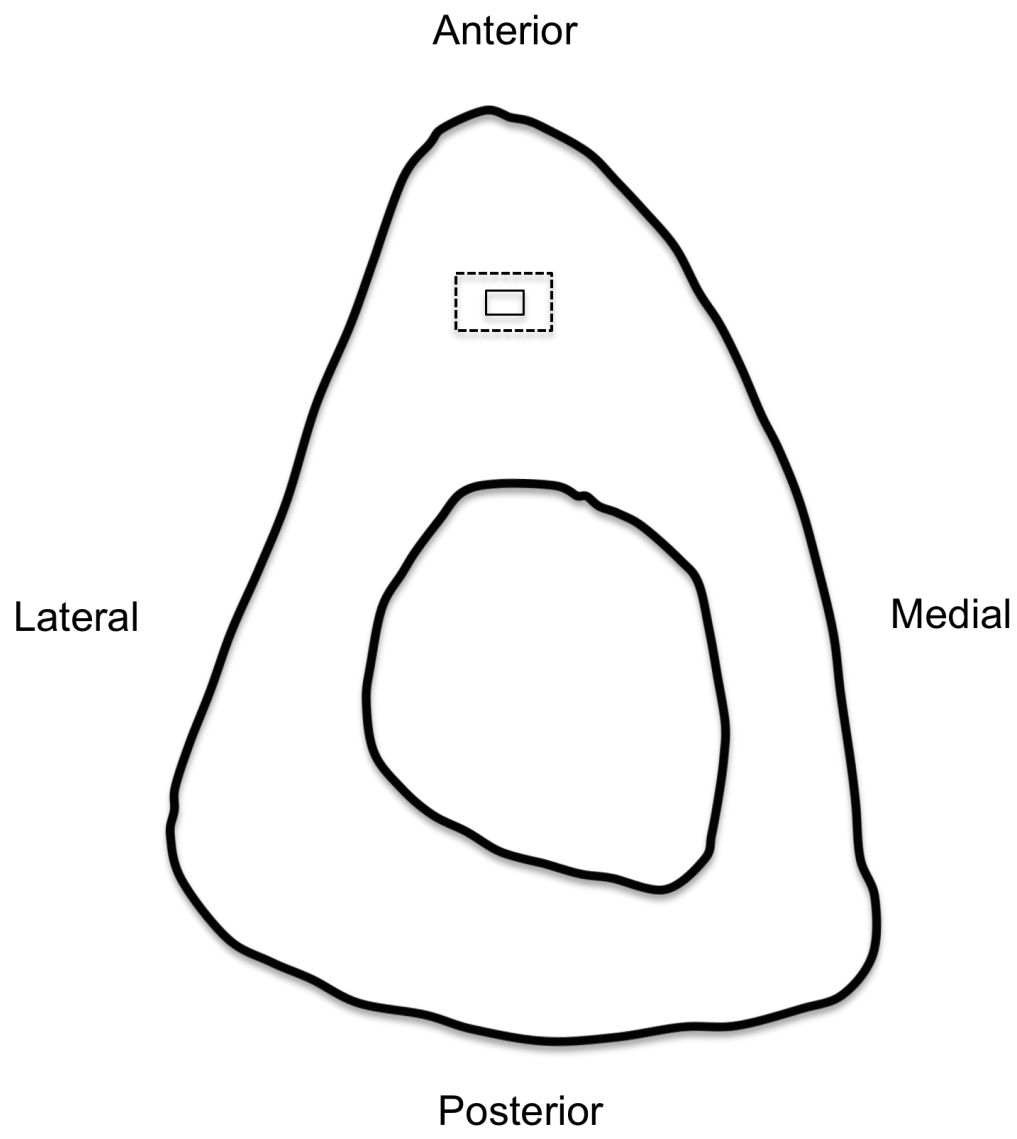


Figure 6. Image capture for data collection comparing magnification level/field size. For each slide, one image at 40x (dashed line) and one at 100x (solid line) magnification were taken from the same area in the midpoint of the anterior cortex. Image not drawn to scale.

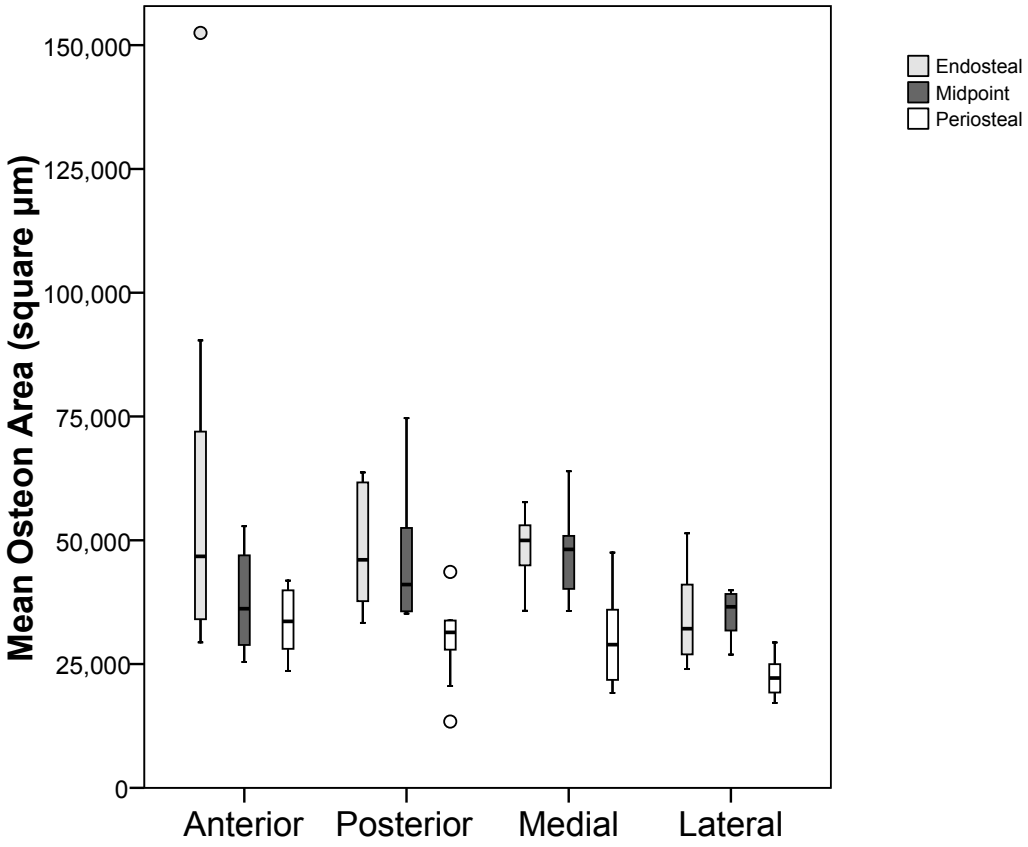


Figure 7. Boxplot of medians and quartiles illustrating a comparison of mean osteon area ($\mu m^2$) between periosteal, endosteal and mid-cortical sampling locations for the anterior, posterior, medial and lateral quadrants. Mean osteon area differed significantly between endosteal, periosteal, and mid-cortical sampling locations in all four quadrants examined.

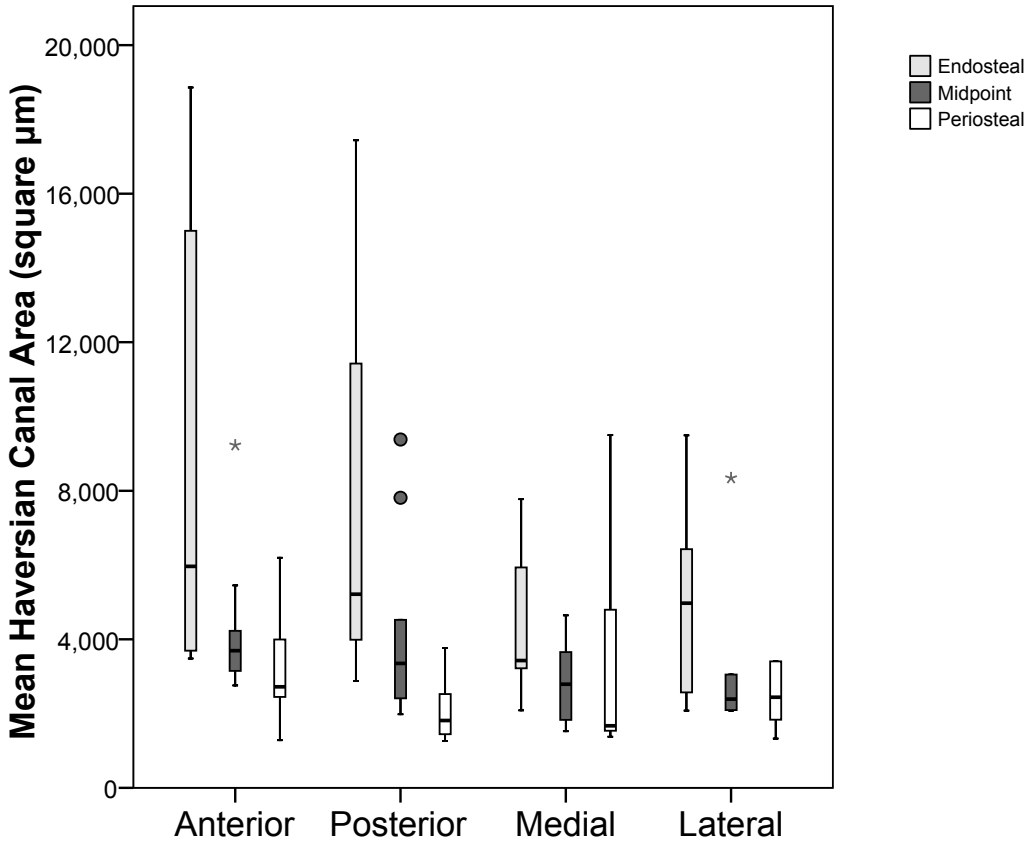


Figure 8. Boxplot of medians and quartiles illustrating a comparison of mean Haversian canal area ($\mu m^2$) between periosteal, endosteal and mid-cortical sampling locations for the anterior, posterior, medial and lateral quadrants. Mean Haversian canal area only differed significantly between endosteal, periosteal, and mid-cortical sampling locations in the posterior quadrant. One extreme outlier has been removed from the anterior endosteal dataset of this graph to improve readability.

.

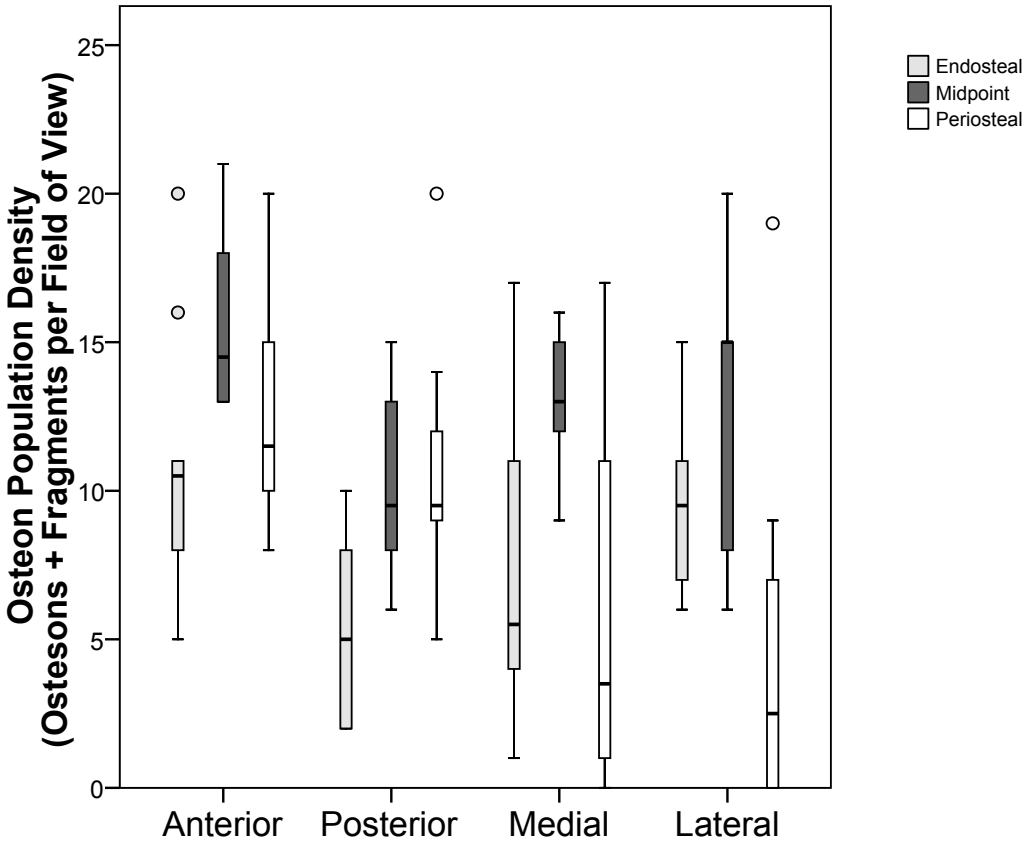


Figure 9. Boxplot of medians and quartiles illustrating a comparison of osteon population density (osteons + osteon fragments per field of view) between periosteal, endosteal and mid-cortical sampling locations for the anterior, posterior, medial and lateral quadrants. OPD differed significantly between endosteal, periosteal, and mid-cortical sampling locations in all four quadrants examined.

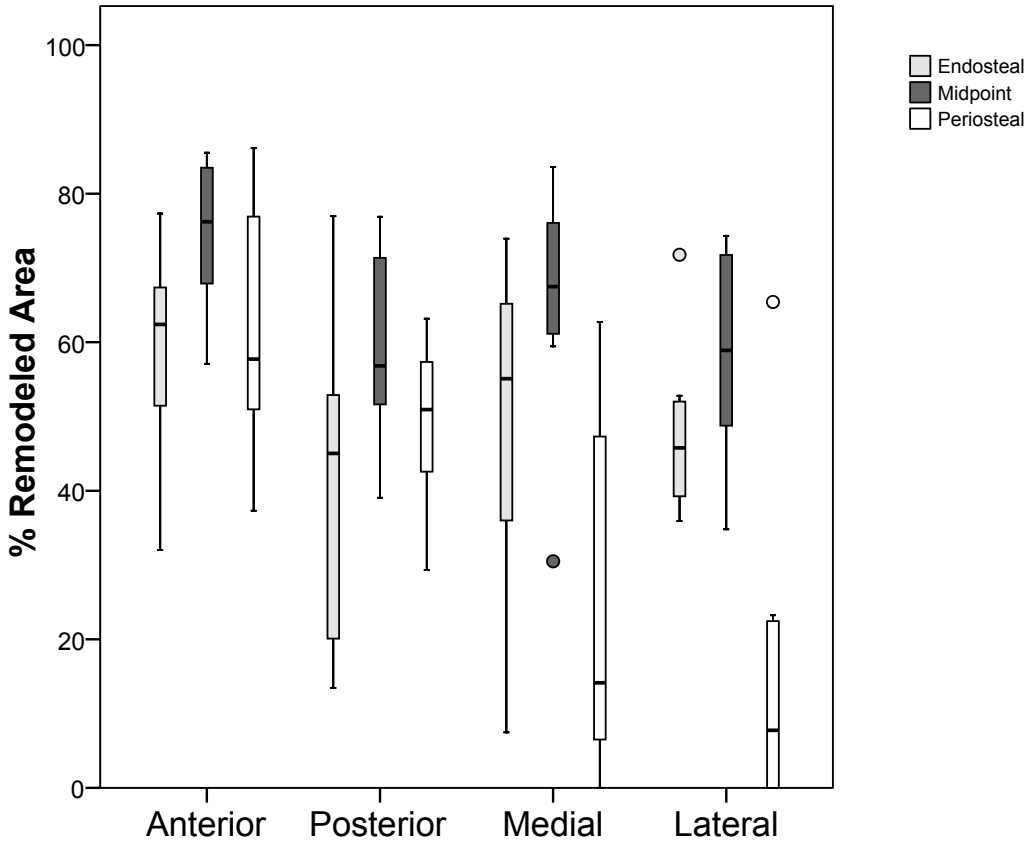


Figure 10. Boxplot of medians and quartiles illustrating a comparison of percent remodeled area between periosteal, endosteal and mid-cortical sampling locations for the anterior, posterior, medial and lateral quadrants. Percent remodeled area differed significantly between endosteal, periosteal, and mid-cortical sampling locations in all four quadrants examined.

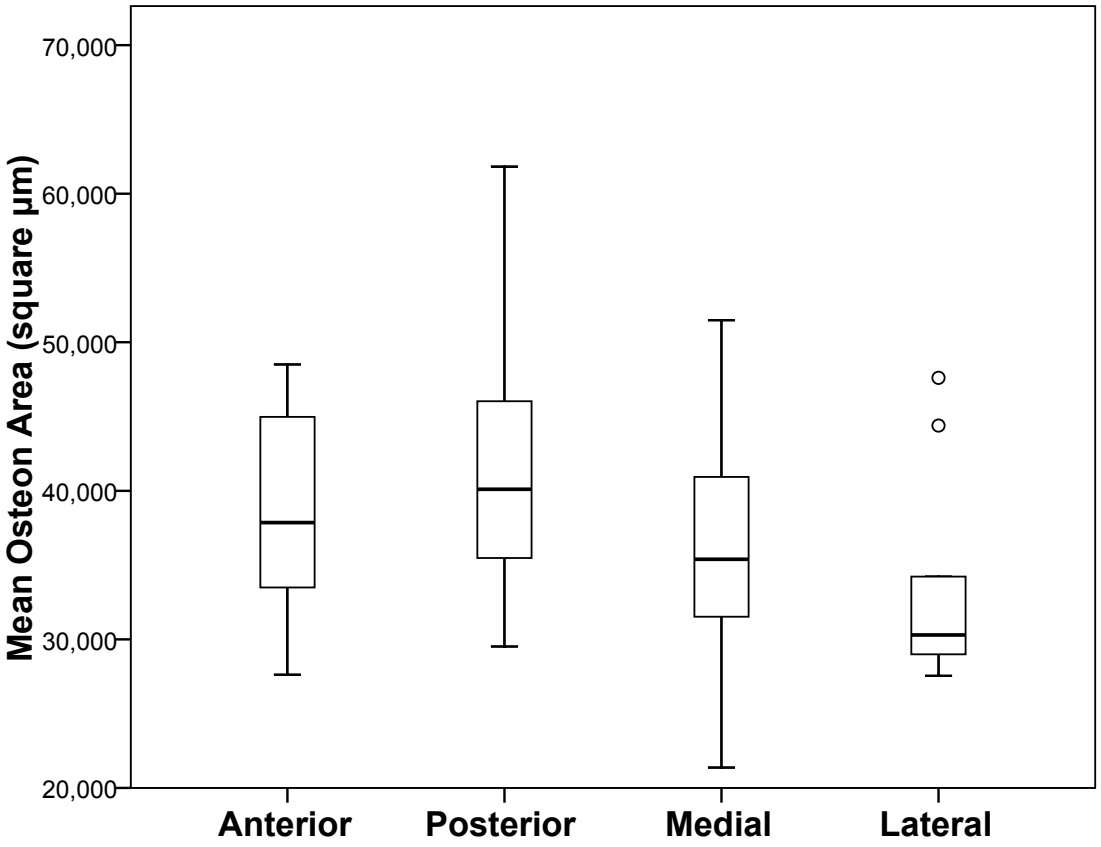


Figure 11. Boxplot of medians and quartiles illustrating a between-slides comparison of mean osteon area ($\mu m^2$). Mean osteon area differed between quadrants ($F = 3.510$, $p = 0.029$) with significantly larger osteons present in the posterior quadrant than the lateral quadrant.

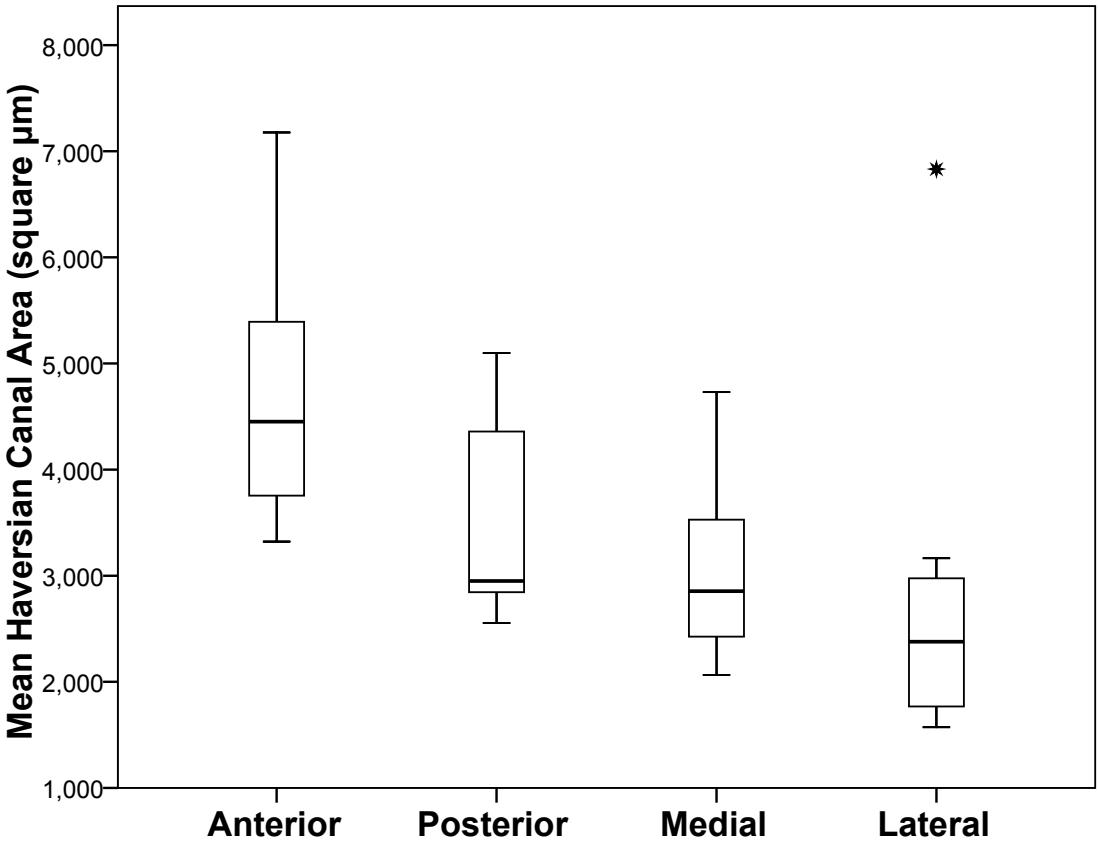


Figure 12. Boxplot of medians and quartiles illustrating a between-slides comparison of mean Haversian canal area ($\mu m^2$). Mean Haversian canal area differed between quadrants ($F = 5.985$, $p = 0.003$).

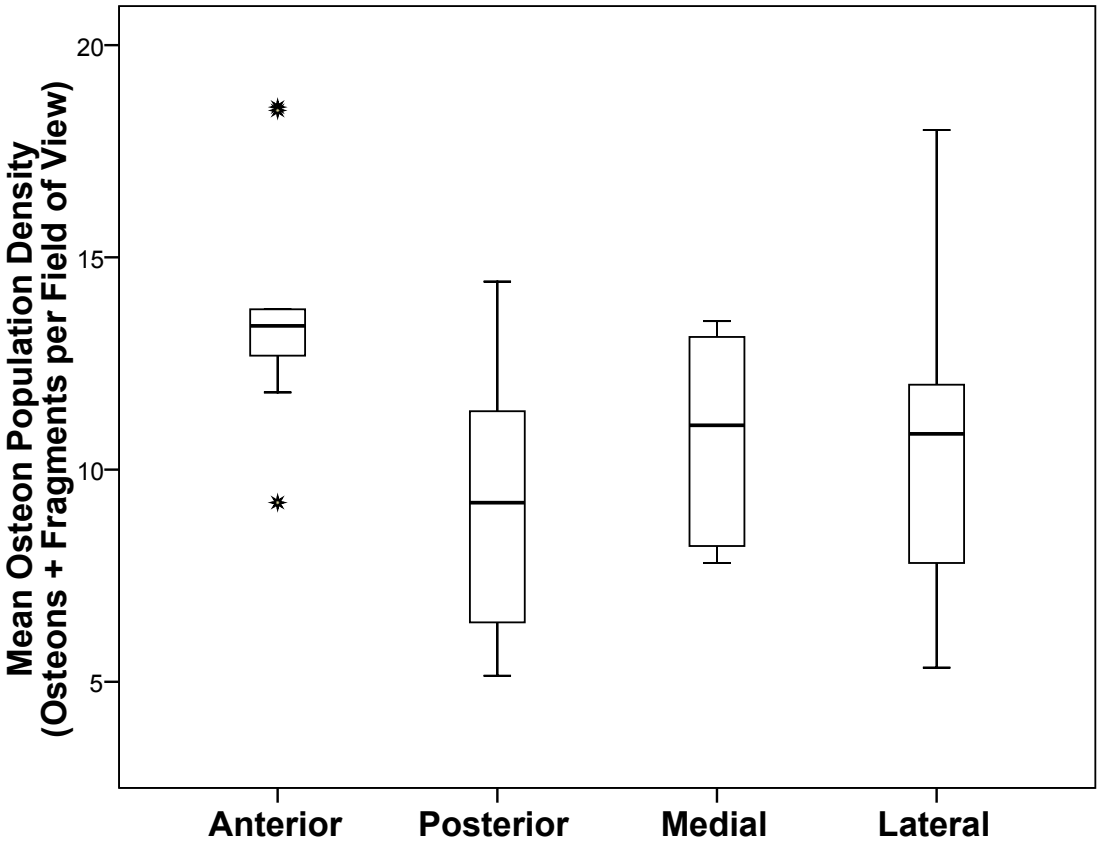


Figure 13. Boxplot of medians and quartiles illustrating a between-slides comparison of OPD (osteons + fragments per field of view). OPD differed between quadrants ($F = 12.042$, $p < 0.001$) with significantly more osteons and osteon fragments present in the anterior quadrant than the posterior and medial quadrants.

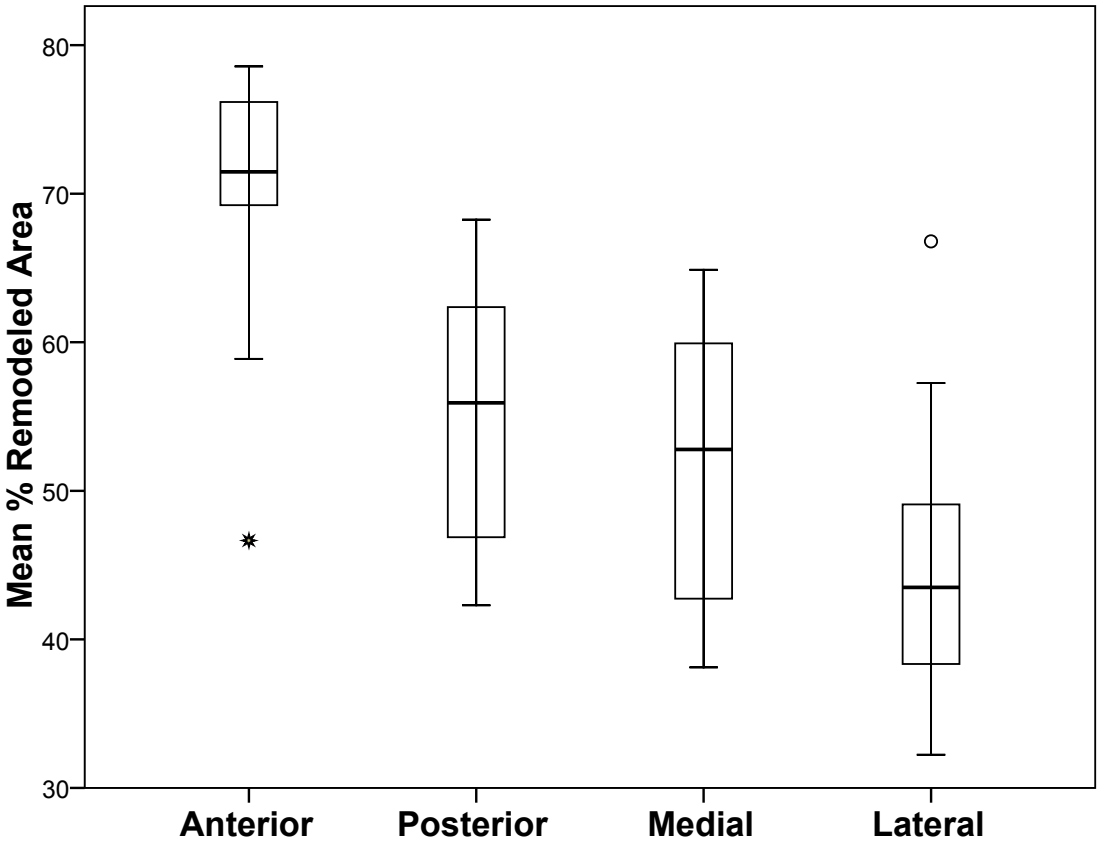


Figure 14. Boxplot of medians and quartiles illustrating a between-slides comparison of mean percent remodeled area. Mean percent remodeled area differed between quadrants ($F = 12.919$, $p < 0.001$) with a significantly greater percent of remodeled area present in the anterior quadrant than the posterior, medial, and lateral quadrants.

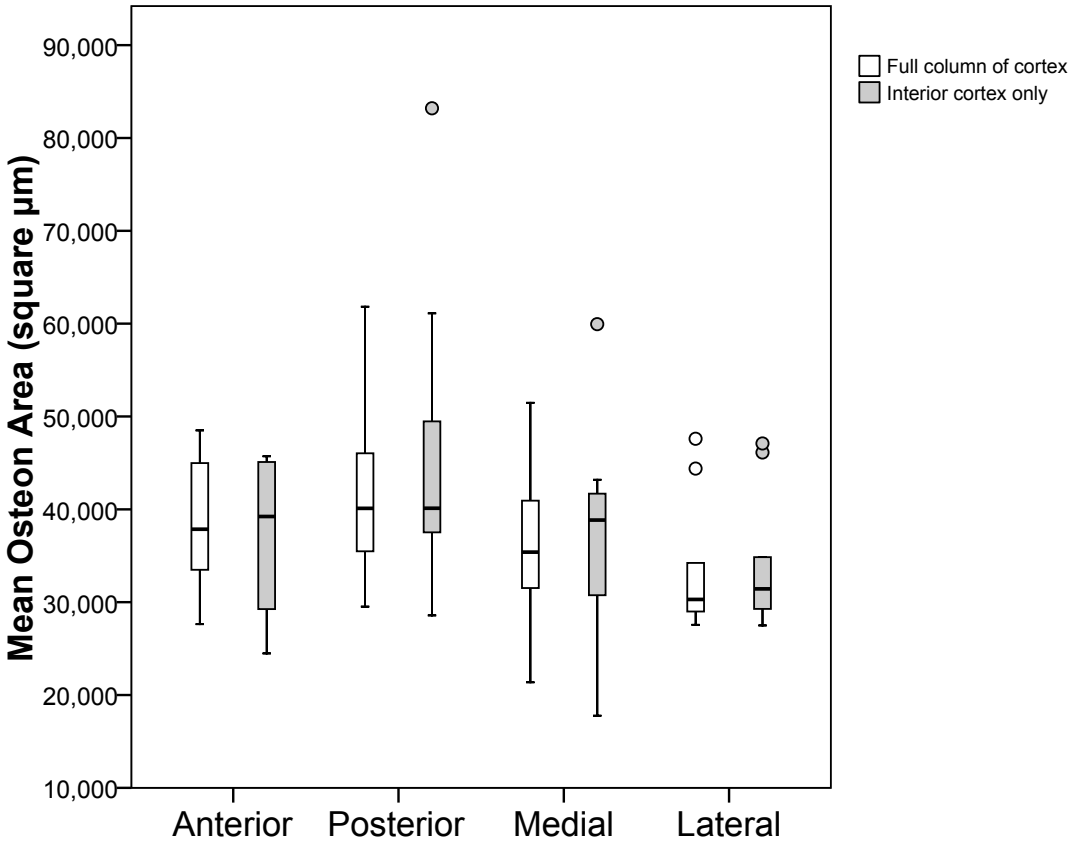


Figure 15. Boxplot of medians and quartiles illustrating a between-slides comparison of mean osteon area ($\mu m^2$) using sampling from the interior cortex only (with a side-by-side comparison of outcomes using the full column of tibial cortex). Mean osteon area differed between quadrants ($F = 2.970$, $p = 0.050$) with significantly larger osteons present in the posterior quadrant than the lateral quadrant.

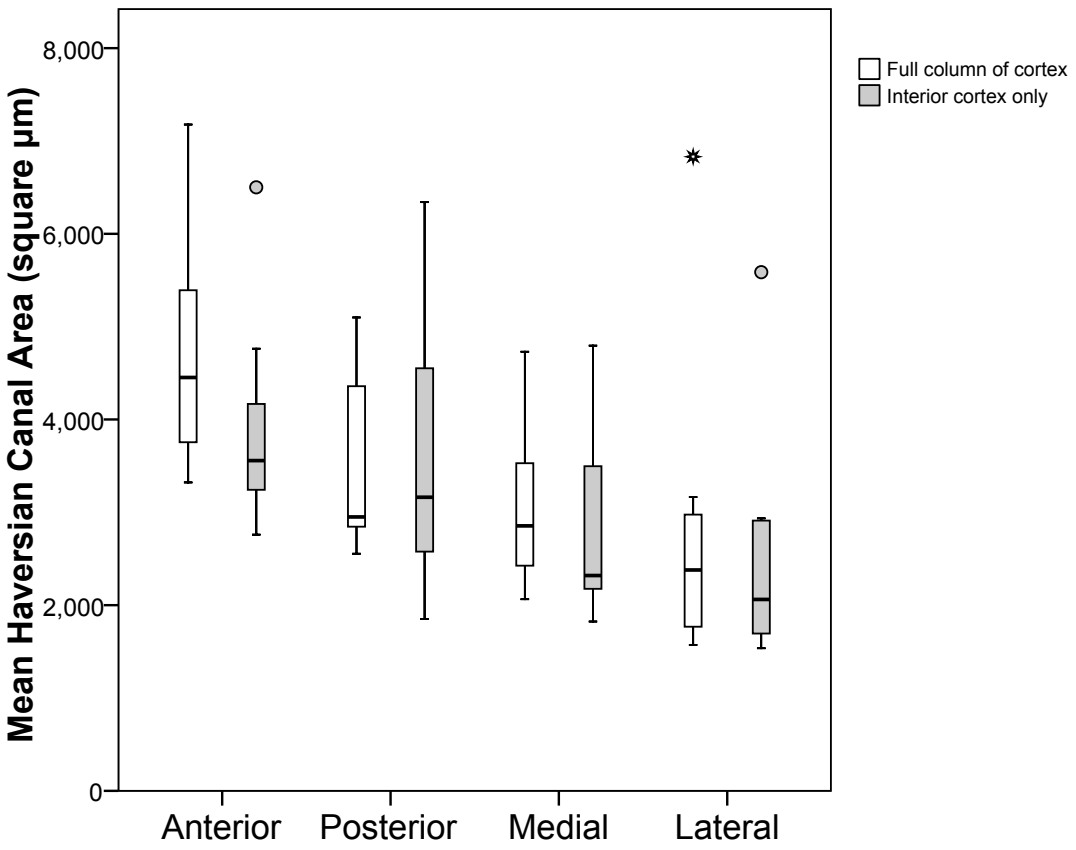


Figure 16. Boxplot of medians and quartiles illustrating a between-slides comparison of mean Haversian canal area ($\mu m^2$) using sampling from the interior cortex only (with a side-by-side comparison of outcomes using the full column of tibial cortex). Mean Haversian canal area differed between quadrants ($F = 4.563$, $p = 0.010$).

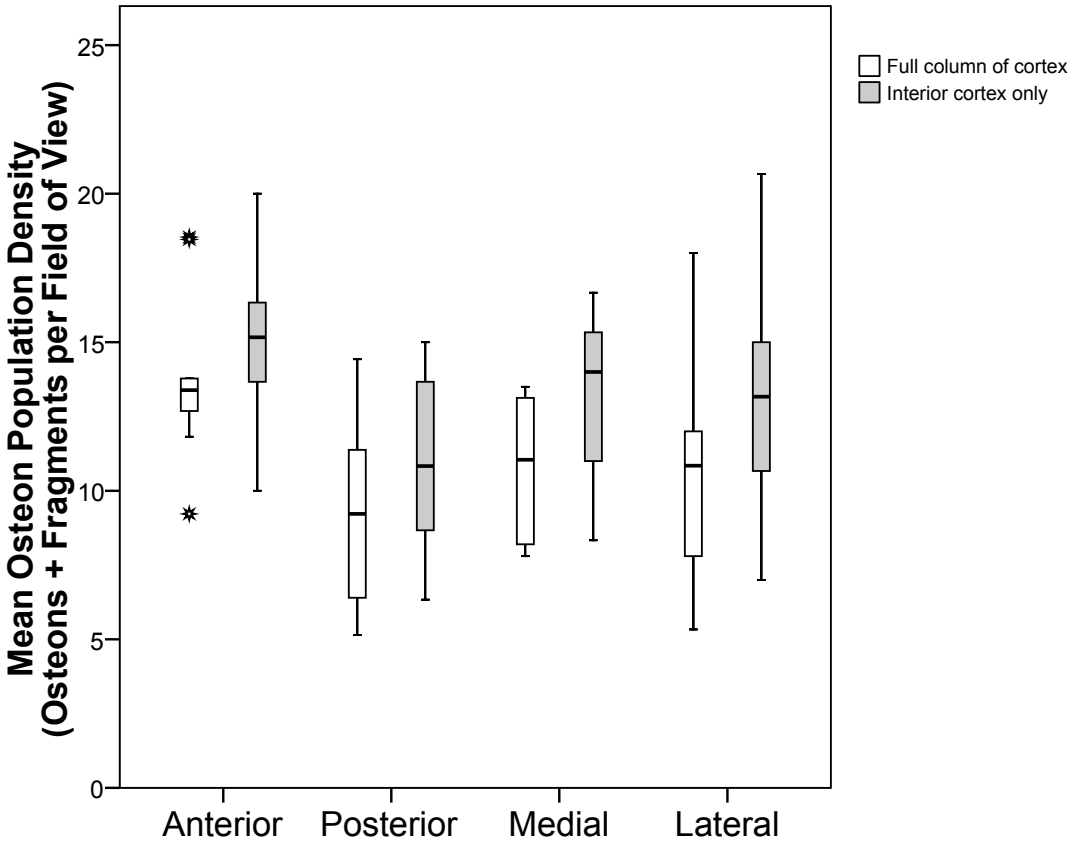


Figure 17. Boxplot of medians and quartiles illustrating a between-slides comparison of OPD (osteons + osteon fragments per field of view) using sampling from the interior cortex only (with a side-by-side comparison of outcomes using the full column of tibial cortex). OPD differed between quadrants ($F = 8.278$, $p < 0.001$) with significantly greater OPD present in the anterior and medial quadrants than the posterior quadrant.

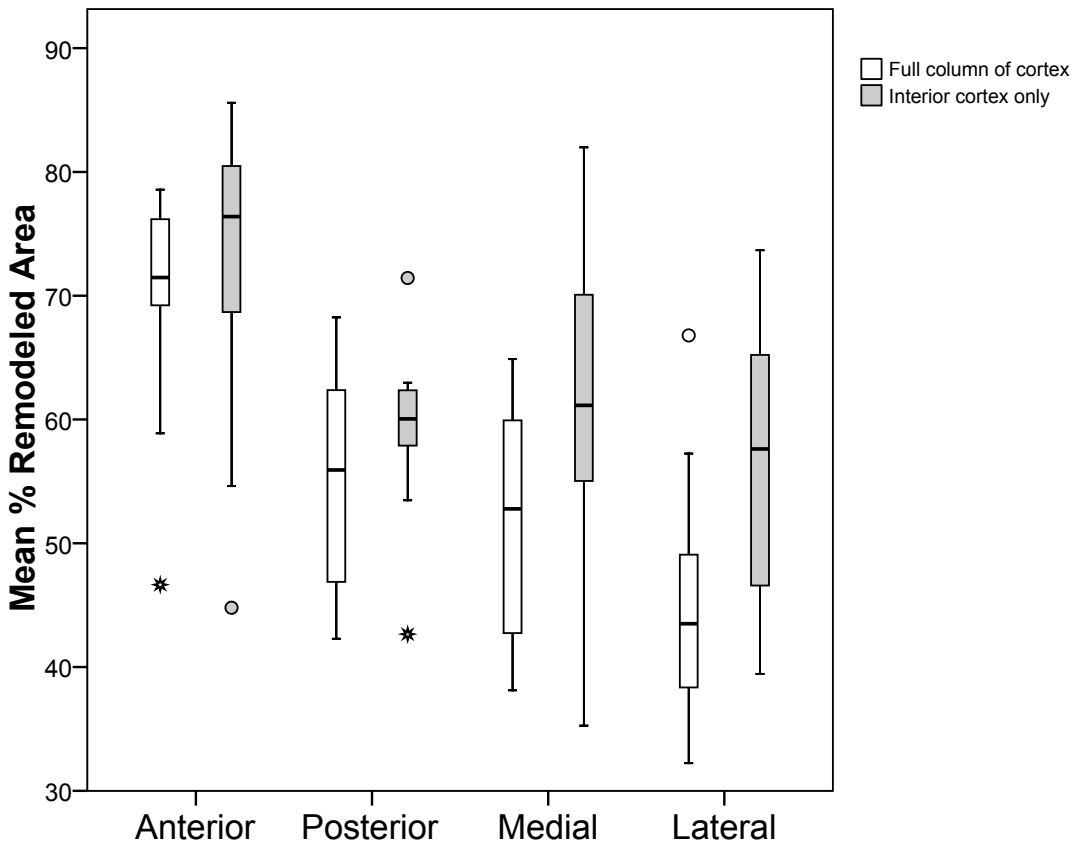


Figure 18. Boxplot of medians and quartiles illustrating a between-slides comparison of percent remodeled area using sampling from the interior cortex only (with a side-by-side comparison of outcomes using the full column of tibial cortex). Percent remodeled area differed between quadrants ($F = 3.361$, $p = 0.033$) with a significantly greater percent of remodeled area present in the anterior quadrant than the posterior quadrant.

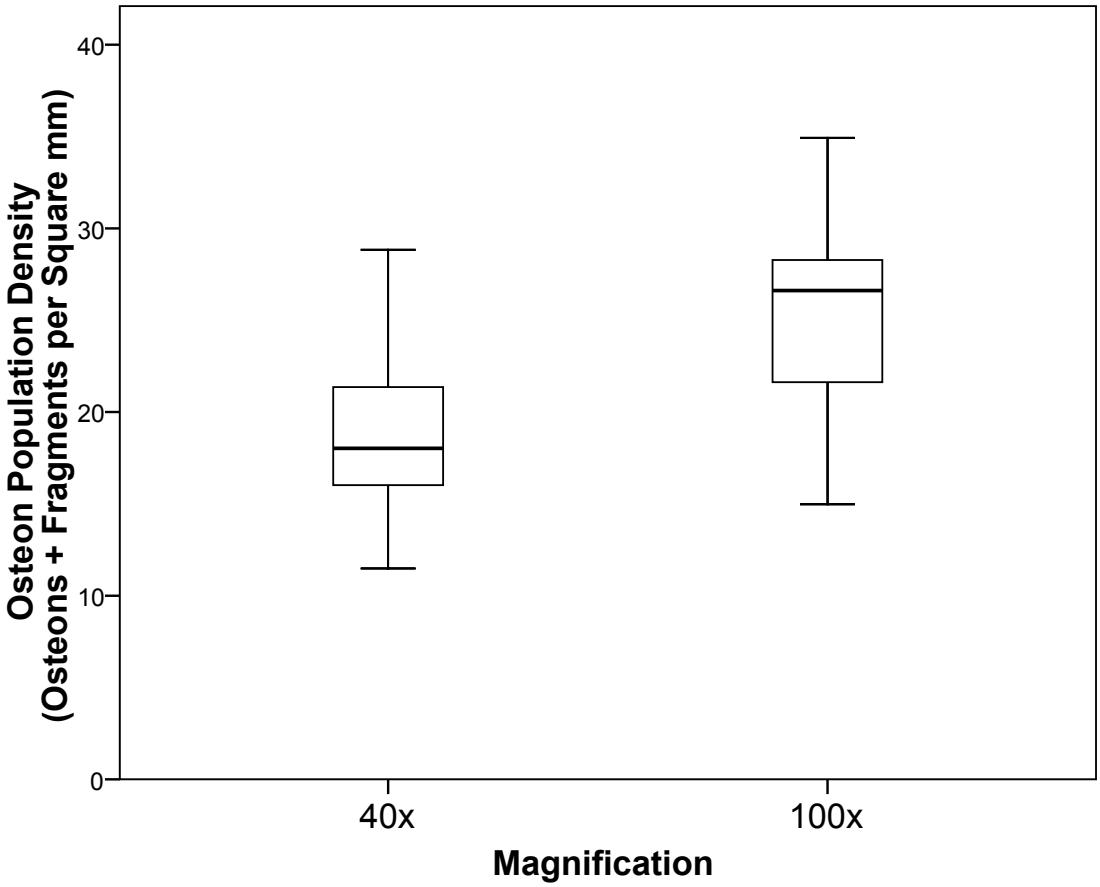


Figure 19. Boxplot of medians and quartiles illustrating a comparison of OPD (osteons + osteon fragments per $mm^2$) at 40x and 100x magnifications. OPD differed between levels of magnification ($t = -4.100$, $p = 0.003$) with a significantly greater density of osteons and fragments present at 100x magnification.

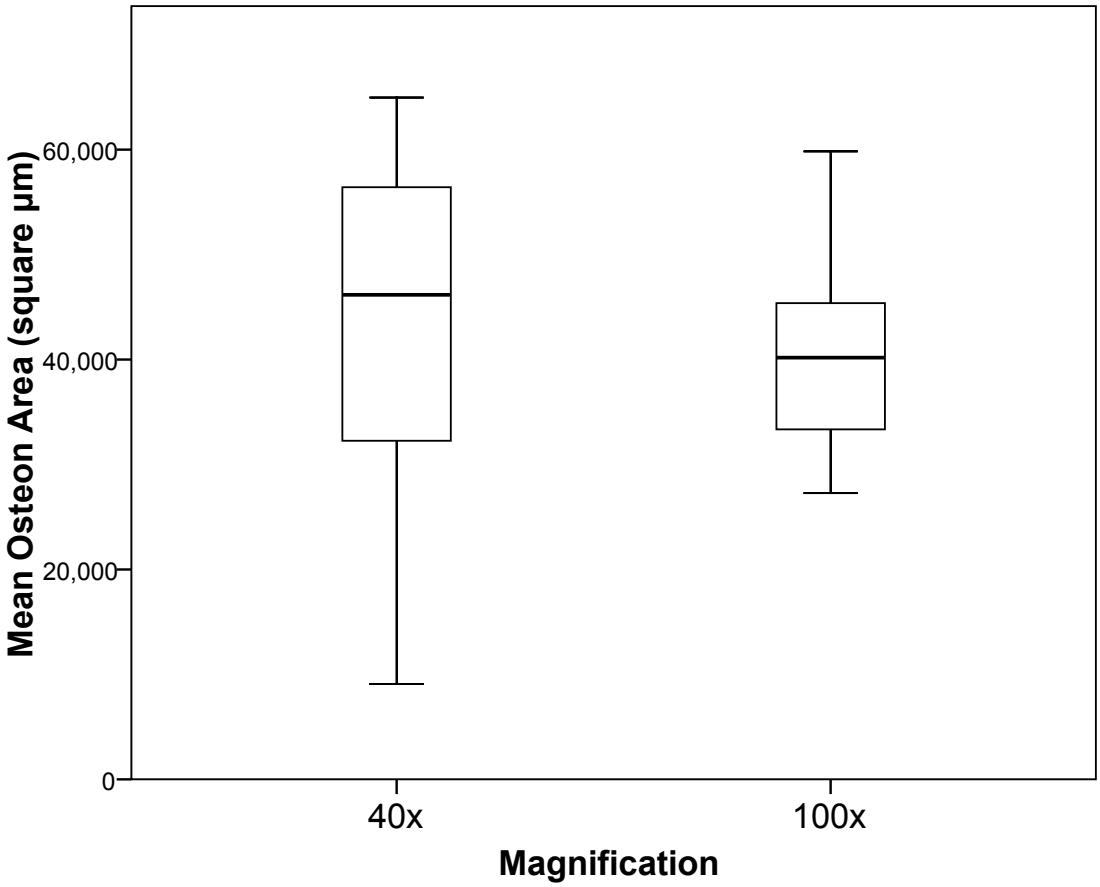


Figure 20. Boxplot of medians and quartiles illustrating a comparison of mean osteon area ($\mu m^2$) at 40x and 100x magnifications. Mean osteon area did not differ significantly between levels of magnification.

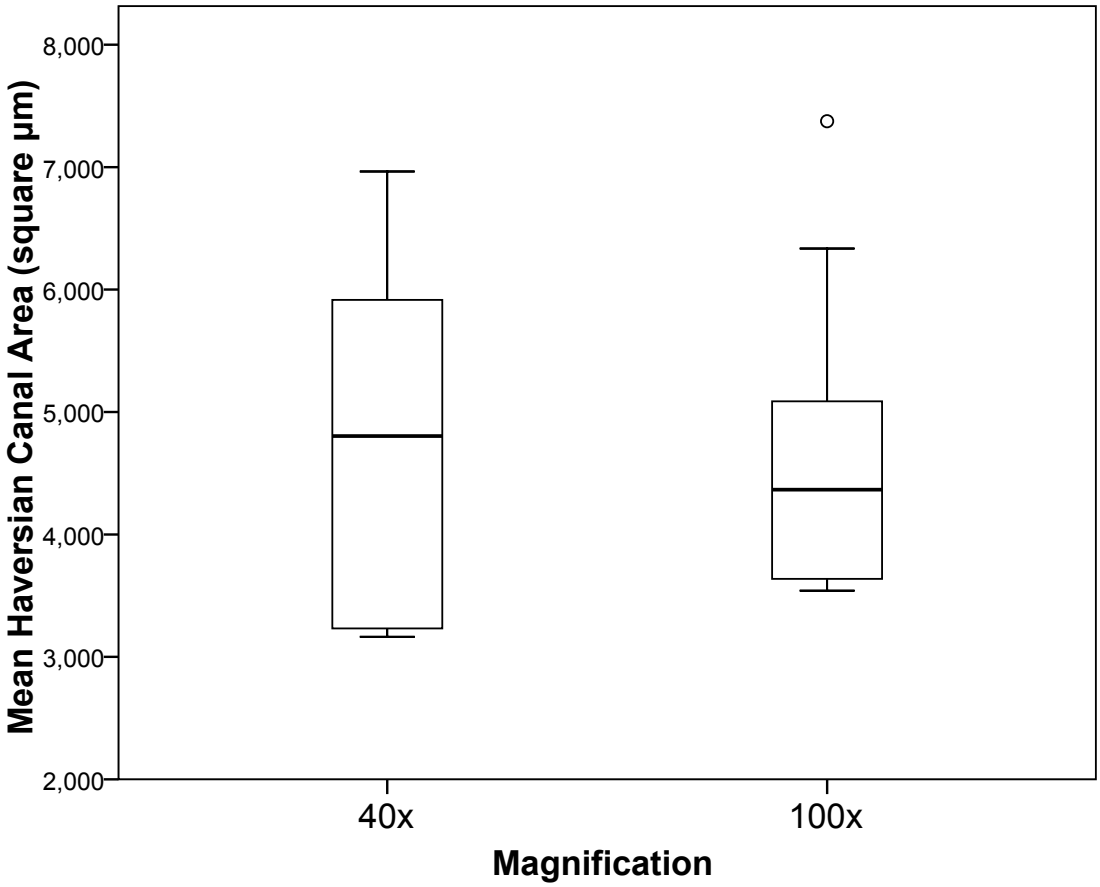


Figure 21. Boxplot of medians and quartiles illustrating a comparison of mean Haversian canal area ($\mu m^2$) at 40x and 100x magnifications. Mean Haversian canal area did not differ significantly between levels of magnification.

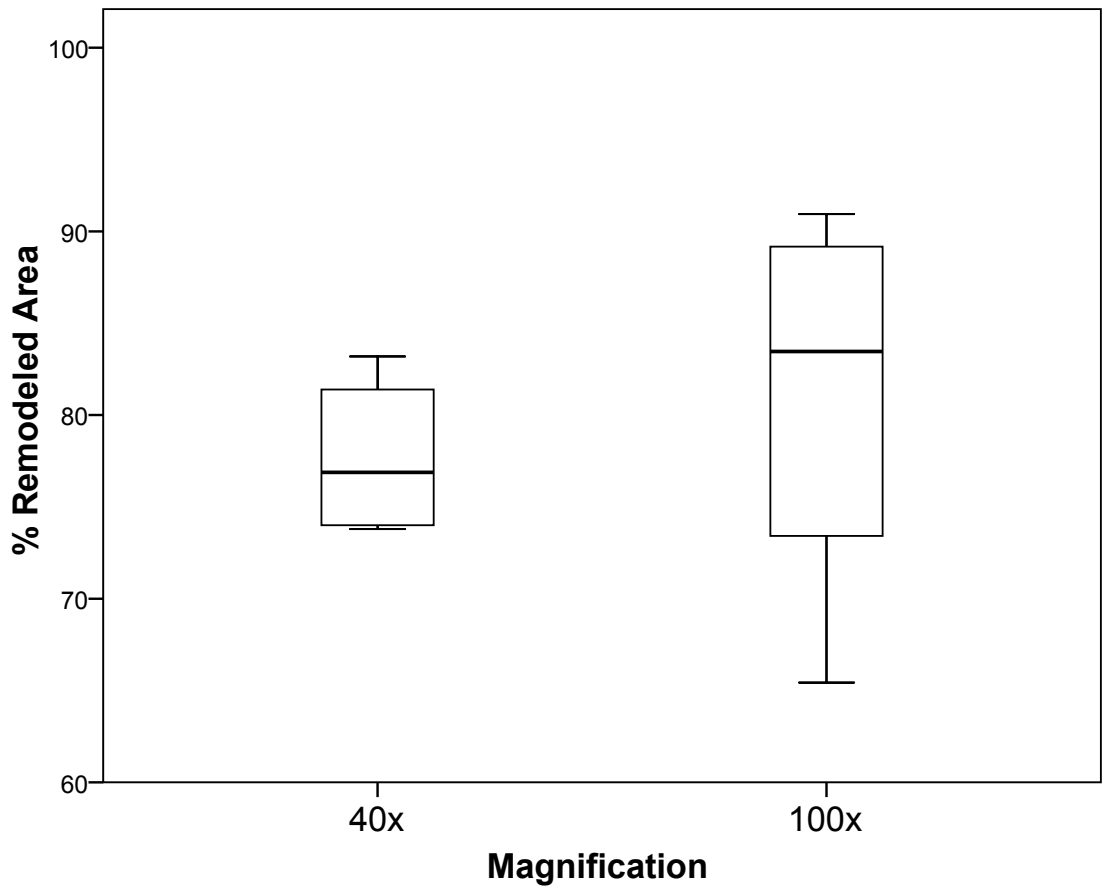


Figure 22. Boxplot of medians and quartiles illustrating a comparison of percent remodeled area at 40x and 100x magnifications. Percent remodeled area did not differ significantly between levels of magnification. One extreme outlier from the 40x magnification has been trimmed from this graph for readability.

**Table 1.**

| Sex | Estimated Age | Race | Slide ID |
|---|---|---|---|
| Female | 20 | White | F011398 |
| Female | 40+ | Black | F072098 |
| Female | 40+ | Black | F100698 |
| Male | 30-40 | White | 10995 |
| Male | 40+ | White | 92297 |
| Male | 20-30 | White | F011691 |
| Male | early 20s | White | F032798 |
| Male | 25-35 | White | F041700 |
| Male | 70+ | ? | F92084 |
| Male | 20-30 | White | Forensic 1-2-81 |

**Table 2.**

| Remodeling Parameter | Description |
|---|---|
| Osteon Area | Osteon area was defined as the area ($\mu m^2$) contained within the cement (reversal) line for each whole osteon within a field of view. Whole osteons were defined as those osteons with a minimum of 90 percent of their Haversian canals intact and within the field of view. This measurement included the area of the Haversian canal. |
| Haversian Canal Area | Haversian canal area was defined as the area ($\mu m^2$) contained within the walls of the Haversian canal of each whole osteon, as defined above. |
| Osteon Population Density (OPD) | Osteon population density consisted of the number of whole osteons plus the number of osteon fragments per field of view. Whole osteons are defined above. Osteon fragments were defined as those osteons exhibiting only a fraction of their original lamellar area and less than 90 percent of the Haversian canal in view either because of encroachment by other osteons or because they were cut off at the edges of the field of view. |
| Percent Remodeled Bone | Percent remodeled bone consisted of the total remodeled area within each field of view (area of whole osteons + area of osteon fragments) expressed as a percent of the total area within each field of view. |

**Table 3. Comparison of Remodeling Variables in the Endosteal Surface, Midpoint, and Periosteal Surface of Each Quadrant with Raw Data**

| Variable | Quadrant | F | p | Descending Magnitude | E x M | E x P | M x P |
|---|---|---|---|---|---|---|---|
| **Osteon Area** | Anterior | 3.865 | 0.040 | E, M, P | ns | ns | ns |
| | Posterior | 9.514 | 0.002 | E, M, P | ns | 0.005 | 0.004 |
| | Medial* | 7.929 | 0.006 | E, M, P | ns | ns | 0.002 |
| | Lateral** | 8.980 | 0.006 | M, E, P | ns | 0.022 | 0.010 |
| **Haversian Canal Area** | Anterior | 2.546 | 0.106 | M, P, E | - | - | - |
| | Posterior | 7.493 | 0.004 | E, M, P | ns | 0.015 | ns |
| | Medial* | 0.814 | 0.466 | E, P, M | - | - | - |
| | Lateral** | 0.593 | 0.571 | E, P, M | - | - | - |
| **OPD** | Anterior | 5.371 | 0.015 | M, P, E | 0.017 | ns | ns |
| | Posterior | 15.260 | <0.001 | P, M, E | 0.008 | 0.003 | ns |
| | Medial | 5.343 | 0.015 | M, E, P | 0.047 | ns | 0.006 |
| | Lateral | 11.474 | 0.001 | M, E, P | ns | ns | 0.003 |
| **% Remodeled Area** | Anterior | 3.845 | 0.041 | M, P, E | ns | ns | 0.039 |
| | Posterior | 4.161 | 0.033 | M, P, E | ns | ns | ns |
| | Medial | 9.380 | 0.002 | M, E, P | ns | ns | <0.001 |
| | Lateral | 27.239 | <0.001 | M, E, P | ns | 0.002 | <0.001 |

E = Endosteal, M = Midpoint, P = Periosteal
Post-hoc analyses were only performed if the results of the repeated measures ANOVA proved significant.
* Slides F011398, F032798, and F92084 had no osteons present in one or more images and were excluded from analysis.
** Slides 10995, 92297, F011691, F032798, and F92084 had no osteons present in one or more images and were excluded from analysis.

**Table 4. Comparison of Remodeling Variables in the Endosteal Surface, Midpoint, and Periosteal Surface of Each Quadrant with Rank-Transformed Data**

| Variable | Quadrant | F | p | Descending Magnitude | E x M | E x P | M x P |
|---|---|---|---|---|---|---|---|
| **Osteon Area** | Anterior | 3.256 | 0.062 | E, M, P | - | - | - |
| | Posterior | 13.671 | <0.001 | E, M, P | ns | 0.003 | 0.003 |
| | Medial* | 10.387 | 0.002 | E, M, P | ns | 0.036 | 0.002 |
| | Lateral** | 10.348 | 0.004 | M, E, P | ns | 0.012 | 0.009 |
| **Haversian Canal Area** | Anterior | 5.517 | 0.014 | E, M, P | ns | 0.035 | ns |
| | Posterior | 23.571 | <0.001 | E, M, P | ns | <0.001 | 0.013 |
| | Medial* | 2.009 | 0.177 | E, M, P | - | - | - |
| | Lateral** | 1.770 | 0.220 | E, M, P | - | - | - |
| **OPD** | Anterior | 6.878 | 0.006 | M, P, E | 0.006 | ns | ns |
| | Posterior | 13.864 | <0.001 | P, M, E | 0.019 | 0.003 | ns |
| | Medial | 5.294 | 0.016 | M, E, P | ns | ns | 0.007 |
| | Lateral | 11.478 | 0.001 | M, E, P | ns | 0.047 | 0.003 |
| **% Remodeled Area** | Anterior | 4.616 | 0.024 | M, P, E | ns | ns | 0.031 |
| | Posterior | 3.791 | 0.042 | M, P, E | ns | ns | ns |
| | Medial | 9.676 | 0.001 | M, E, P | ns | ns | <0.001 |
| | Lateral | 18.775 | <0.001 | M, E, P | ns | 0.006 | 0.001 |

E = Endosteal, M = Midpoint, P = Periosteal
Post-hoc analyses were only performed if the results of the repeated measures ANOVA proved significant.
* Slides F011398, F032798, and F92084 had no osteons present in one or more images and were excluded from analysis.
** Slides 10995, 92297, F011691, F032798, and F92084 had no osteons present in one or more images and were excluded from analysis.

**Table 5. Within-Slide Comparison of Osteon Area Using the Entire Endosteal to Periosteal Column of Cortex with Raw Data**

| | *Repeated Measures ANOVA* | | | *Post-hoc Pairwise Comparisons* | | | | | |
|---|---|---|---|---|---|---|---|---|---|
| **Slide ID** | **F** | **p** | **Descending Magnitude** | **A x P** | **A x M** | **A x L** | **P x M** | **P x L** | **M x L** |
| 10995 | 1.878 | 0.133 | A, P, M, L | - | - | - | - | - | - |
| 92297 | 1.429 | 0.237 | P, L, A, M | - | - | - | - | - | - |
| F011398 | 6.269 | <0.001 | P, M, A, L | ns | ns | ns | ns | 0.002 | ns |
| F011691 | 0.105 | 0.957 | A, P, M, L | - | - | - | - | - | - |
| F032798 | 18.909 | <0.001 | A, P, L, M | ns | <0.001 | <0.001 | <0.001 | 0.003 | 0.014 |
| F041700 | 4.286 | 0.006 | A, P, M, L | ns | ns | <0.001 | ns | 0.006 | ns |
| F072098 | 5.563 | 0.001 | P, M, L, A | 0.033 | ns | ns | ns | ns | ns |
| F92084 | 0.105 | 0.957 | L, P, M, A | - | - | - | - | - | - |
| F100698 | 3.933 | 0.009 | A, M, P, L | ns | ns | 0.001 | ns | ns | ns |
| Forensic 1-2-81 | 1.627 | 0.183 | P, M, L, A | - | - | - | - | - | - |

A = Anterior, P = Posterior, M = Medial, L = Lateral
Post-hoc analyses were only performed if the results of the repeated measures ANOVA proved significant.

**Table 6. Within-Slide Comparison of Haversian Canal Areas Using the Entire Endosteal to Periosteal Column of Cortex with Raw Data**

| | *Repeated Measures ANOVA* | | | *Post-hoc Pairwise Comparisons* | | | | | |
|---|---|---|---|---|---|---|---|---|---|
| **Slide ID** | **F** | **p** | **Descending Magnitude** | **A x P** | **A x M** | **A x L** | **P x M** | **P x L** | **M x L** |
| 10995 | 3.362 | 0.019 | A, M, P, L | 0.038 | ns | 0.002 | ns | 0.006 | ns |
| 92297 | 1.023 | 0.384 | A, P, M, L | - | - | - | - | - | - |
| F011398 | 14.221 | <0.001 | P, A, M, L | ns | ns | <0.001 | 0.013 | <0.001 | ns |
| F011691 | 4.341 | 0.005 | A, P, L, M | ns | 0.010 | <0.001 | ns | ns | ns |
| F032798 | 3.707 | 0.012 | A, P, M, L | ns | 0.003 | <0.001 | ns | ns | ns |
| F041700 | 15.185 | <0.001 | A, P, M, L | <0.001 | <0.001 | <0.001 | ns | 0.022 | ns |
| F072098 | 1.960 | 0.122 | L, P, M, A | - | - | - | - | - | - |
| F92084 | 2.659 | 0.048 | A, L, M, P | 0.030 | ns | ns | ns | ns | ns |
| F100698 | 2.567 | 0.056 | A, M, P, L | - | - | - | - | - | - |
| Forensic 1-2-81 | 1.169 | 0.321 | M, P, A, L | - | - | - | - | - | - |

A = Anterior, P = Posterior, M = Medial, L = Lateral
Post-hoc analyses were only performed if the results of the repeated measures ANOVA proved significant.

**Table 7. Within-Slide Comparison of Osteon Population Density Using the Entire Endosteal to Periosteal Column of Cortex with Raw Data**

| | *Repeated Measures ANOVA* | | | *Post-hoc Pairwise Comparisons* | | | | | |
|---|---|---|---|---|---|---|---|---|---|
| **Slide ID** | **F** | **p** | **Descending Magnitude** | **A x P** | **A x M** | **A x L** | **P x M** | **P x L** | **M x L** |
| 10995 | 0.914 | 0.443 | A, P, M, L | - | - | - | - | - | - |
| 92297 | 3.110 | 0.046 | A, M, L, P | 0.007 | ns | ns | ns | ns | ns |
| F011398 | 2.805 | 0.060 | L, A, M/P | - | - | - | - | - | - |
| F011691 | 8.583 | <0.001 | A, M, P, L | 0.001 | ns | ns | ns | ns | ns |
| F032798 | 0.765 | 0.521 | A, M, L, P | - | - | - | - | - | - |
| F041700 | 2.763 | 0.062 | A, M, L, P | - | - | - | - | - | - |
| F072098 | 14.581 | <0.001 | A, M, P, L | <0.001 | ns | 0.004 | ns | ns | ns |
| F92084 | 2.275 | 0.103 | A, L, P, M | - | - | - | - | - | - |
| F100698 | 0.614 | 0.611 | A, M, L, P | - | - | - | - | - | - |
| Forensic 1-2-81 | 2.757 | 0.059 | A, M, P, L | - | - | - | - | - | - |

A = Anterior, P = Posterior, M = Medial, L = Lateral
Post-hoc analyses were only performed if the results of the repeated measures ANOVA proved significant.

**Table 8. Within-Slide Comparison of Percent Remodeled Area Using the Entire Endosteal to Periosteal Column of Cortex with Raw Data**

| | *Repeated Measures ANOVA* | | | *Post-hoc Pairwise Comparisons* | | | | | |
|---|---|---|---|---|---|---|---|---|---|
| **Slide ID** | **F** | **p** | **Descending Magnitude** | **A x P** | **A x M** | **A x L** | **P x M** | **P x L** | **M x L** |
| 10995 | 7.009 | 0.001 | A, P, M, L | ns | ns | ns | ns | ns | ns |
| 92297 | 4.541 | 0.012 | A, P, M, L | 0.012 | ns | ns | ns | ns | ns |
| F011398 | 0.667 | 0.580 | L, M, A, P | - | - | - | - | - | - |
| F011691 | 13.017 | <0.001 | A, P, M, L | 0.001 | ns | 0.045 | ns | ns | ns |
| F032798 | 15.118 | <0.001 | A, P, L, M | ns | 0.033 | ns | ns | ns | ns |
| F041700 | 4.878 | 0.008 | A, M, P, L | ns | ns | 0.022 | ns | ns | ns |
| F072098 | 2.949 | 0.052 | A, M, P, L | - | - | - | - | - | - |
| F92084 | 2.444 | 0.086 | A, L, P, M | - | - | - | - | - | - |
| F100698 | 5.836 | 0.003 | A, M, P, L | 0.015 | ns | ns | ns | ns | ns |
| Forensic 1-2-81 | 2.804 | 0.056 | A, M, L, P | - | - | - | - | - | - |

A = Anterior, P = Posterior, M = Medial, L = Lateral
Post-hoc analyses were only performed if the results of the repeated measures ANOVA proved significant.

**Table 9. Within-Slide Comparison of Osteon Area Using the Entire Endosteal to Periosteal Column of Cortex with Rank-Transformed Data**

| | *Repeated Measures ANOVA* | | | *Post-hoc Pairwise Comparisons* | | | | | |
|---|---|---|---|---|---|---|---|---|---|
| **Slide ID** | **F** | **p** | **Descending Magnitude** | **A x P** | **A x M** | **A x L** | **P x M** | **P x L** | **M x L** |
| 10995 | 2.054 | 0.106 | A, P, M, L | - | - | - | - | - | - |
| 92297 | 3.075 | 0.030 | P, L, M, A | 0.036 | ns | ns | ns | ns | ns |
| F011398 | 5.301 | 0.002 | P, A, M, L | ns | ns | ns | ns | 0.001 | ns |
| F011691 | 0.199 | 0.897 | L, P, A, M | - | - | - | - | - | - |
| F032798 | 22.014 | <0.001 | P, A, L, M | ns | <0.001 | 0.003 | <0.001 | 0.011 | 0.009 |
| F041700 | 4.544 | 0.004 | A, P, M, L | ns | ns | <0.001 | ns | 0.012 | ns |
| F072098 | 5.087 | 0.002 | P, M, L, A | 0.012 | ns | ns | ns | ns | ns |
| F92084 | 0.596 | 0.618 | L, P, M, A | - | - | - | - | - | - |
| F100698 | 5.050 | 0.002 | A, M, P, L | ns | ns | 0.001 | ns | ns | ns |
| Forensic 1-2-81 | 1.026 | 0.381 | P, L, M, A | - | - | - | - | - | - |

A = Anterior, P = Posterior, M = Medial, L = Lateral
Post-hoc analyses were only performed if the results of the repeated measures ANOVA proved significant.

**Table 10. Within-Slide Comparison of Haversian Canal Areas Using the Entire Endosteal to Periosteal Column of Cortex with Rank-Transformed Data**

| | *Repeated Measures ANOVA* | | | *Post-hoc Pairwise Comparisons* | | | | | |
|---|---|---|---|---|---|---|---|---|---|
| **Slide ID** | **F** | **p** | **Descending Magnitude** | **A x P** | **A x M** | **A x L** | **P x M** | **P x L** | **M x L** |
| 10995 | 8.574 | < 0.001 | A, M, P, L | ns | ns | <0.001 | ns | 0.041 | 0.003 |
| 92297 | 1.614 | 0.189 | P, A, M, L | - | - | - | - | - | - |
| F011398 | 16.491 | <0.001 | P, A, M, L | ns | ns | <0.001 | 0.003 | <0.001 | ns |
| F011691 | 3.337 | 0.020 | A, P, L, M | ns | 0.021 | ns | ns | ns | ns |
| F032798 | 4.202 | 0.006 | A, P, M, L | ns | 0.030 | 0.013 | ns | ns | ns |
| F041700 | *11.782* | <0.001 | *A, P, M, L* | 0.007 | <0.001 | <0.001 | ns | ns | ns |
| F072098 | 2.010 | 0.115 | L, M, P, A | - | - | - | - | - | - |
| F92084 | 3.012 | 0.030 | A, M, P, L | ns | ns | 0.049 | ns | ns | ns |
| F100698 | 7.840 | <0.001 | A, M, P, L | 0.002 | 0.015 | 0.001 | ns | ns | ns |
| Forensic 1-2-81 | 1.564 | 0.198 | P, A, L, M | - | - | - | - | - | - |

A = Anterior, P = Posterior, M = Medial, L = Lateral
Post-hoc analyses were only performed if the results of the repeated measures ANOVA proved significant.

**Table 11. Within-Slide Comparison of Osteon Population Density Using the Entire Endosteal to Periosteal Column of Cortex with Rank-Transformed Data**

| | *Repeated Measures ANOVA* | | | *Post-hoc Pairwise Comparisons* | | | | | |
|---|---|---|---|---|---|---|---|---|---|
| **Slide ID** | **F** | **p** | **Descending Magnitude** | **A x P** | **A x M** | **A x L** | **P x M** | **P x L** | **M x L** |
| 10995 | 0.512 | 0.677 | A, P, L, M | - | - | - | - | - | - |
| 92297 | 2.996 | 0.052 | A, M, L, P | 0.022 | ns | ns | ns | ns | ns |
| F011398 | 2.434 | 0.089 | L, A, M, P | - | - | - | - | - | - |
| F011691 | 9.415 | <0.001 | A, M, P, L | <0.001 | ns | ns | ns | ns | ns |
| F032798 | 0.784 | 0.511 | M, A, L, P | - | - | - | - | - | - |
| F041700 | 4.090 | 0.017 | A, M, L, P | 0.014 | ns | ns | ns | ns | ns |
| F072098 | 18.752 | <0.001 | A, M, P, L | <0.001 | ns | 0.001 | ns | ns | ns |
| F92084 | 3.243 | 0.037 | L, A, M, P | ns | ns | ns | ns | ns | ns |
| F100698 | 0.613 | 0.612 | A, M, L, P | - | - | - | - | - | - |
| Forensic 1-2-81 | 2.213 | 0.106 | A, M, P, L | - | - | - | - | - | - |

A = Anterior, P = Posterior, M = Medial, L = Lateral
Post-hoc analyses were only performed if the results of the repeated measures ANOVA proved significant.

**Table 12. Within-Slide Comparison of Percent Remodeled Area Using the Entire Endosteal to Periosteal Column of Cortex with Rank-Transformed Data**

| | *Repeated Measures ANOVA* | | | *Post-hoc Pairwise Comparisons* | | | | | |
|---|---|---|---|---|---|---|---|---|---|
| **Slide ID** | **F** | **p** | **Descending Magnitude** | **A x P** | **A x M** | **A x L** | **P x M** | **P x L** | **M x L** |
| 10995 | 6.391 | 0.001 | A, P, M, L | ns | ns | 0.001 | ns | 0.031 | ns |
| 92297 | 5.705 | 0.005 | A, P, L, M | 0.002 | ns | ns | ns | ns | ns |
| F011398 | 0.985 | 0.416 | L, M, A, P | - | - | - | - | - | - |
| F011691 | 21.764 | <0.001 | A, M, P, L | <0.001 | ns | 0.003 | ns | ns | ns |
| F032798 | 15.543 | <0.001 | A, P, M, L | 0.018 | 0.005 | <0.001 | ns | ns | ns |
| F041700 | 6.340 | 0.002 | A, M, P, L | ns | ns | <0.001 | ns | ns | ns |
| F072098 | 2.542 | 0.079 | A, M, P, L | - | - | - | - | - | - |
| F92084 | 2.843 | 0.056 | A, L, M, P | - | - | - | - | - | - |
| F100698 | 7.992 | 0.001 | A, M, P, L | 0.003 | ns | 0.003 | ns | ns | ns |
| Forensic 1-2-81 | 4.189 | 0.013 | A, M, P, L | ns | ns | 0.034 | ns | ns | ns |

A = Anterior, P = Posterior, M = Medial, L = Lateral
Post-hoc analyses were only performed if the results of the repeated measures ANOVA proved significant.

## Table 13. Within-Slide Comparison of Osteon Area Using Interior Cortex Only with Raw Data

| | *Repeated Measures ANOVA* | | | *Post-hoc Pairwise Comparisons* | | | | | |
|---|---|---|---|---|---|---|---|---|---|
| **Slide ID** | **F** | **p** | **Descending Magnitude** | **A x P** | **A x M** | **A x L** | **P x M** | **P x L** | **M x L** |
| 10995 | 3.361 | 0.023 | A, P, M, L | ns | ns | 0.003 | ns | ns | ns |
| 92297 | 1.921 | 0.134 | P, L, A, M | - | - | - | - | - | - |
| F011398 | 2.073 | 0.112 | P, M, A, L | - | - | - | - | - | - |
| F011691 | 0.648 | 0.587 | P, L, A, M | - | - | - | - | - | - |
| F032798 | 12.735 | <0.001 | A, P, L, M | ns | <0.001 | ns | <0.001 | ns | <0.001 |
| F041700 | 2.572 | 0.060 | P, A, M, L | - | - | - | - | - | - |
| F072098 | 7.732 | <0.001 | P, M, L, A | 0.014 | ns | ns | ns | ns | ns |
| F92084 | 1.205 | 0.311 | L, M, P, A | - | - | - | - | - | - |
| F100698 | 2.348 | 0.078 | A, M, P, L | - | - | - | - | - | - |
| Forensic 1-2-81 | 1.300 | 0.278 | P, L, M A | - | - | - | - | - | - |

A = Anterior, P = Posterior, M = Medial, L = Lateral
Post-hoc analyses were only performed if the results of the repeated measures ANOVA proved significant.

## Table 14. Within-Slide Comparison of Haversian Canal Area Using Interior Cortex Only with Raw Data

| | *Repeated Measures ANOVA* | | | *Post-hoc Pairwise Comparisons* | | | | | |
|---|---|---|---|---|---|---|---|---|---|
| **Slide ID** | **F** | **p** | **Descending Magnitude** | **A x P** | **A x M** | **A x L** | **P x M** | **P x L** | **M x L** |
| 10995 | 7.442 | <0.001 | A, M, P, L | ns | ns | 0.004 | ns | ns | 0.008 |
| 92297 | 3.436 | 0.021 | A, P, M, L | ns | ns | ns | ns | ns | ns |
| F011398 | 7.797 | <0.001 | P, A, M, L | ns | ns | ns | ns | 0.013 | ns |
| F011691 | 1.659 | 0.183 | A, P, L, M | - | - | - | - | - | - |
| F032798 | 2.407 | 0.072 | A, L, M, P | - | - | - | - | - | - |
| F041700 | 12.372 | <0.001 | A, P, M, L | 0.033 | 0.003 | 0.001 | ns | 0.031 | ns |
| F072098 | 0.227 | 0.877 | L, P, M, A | - | - | - | - | - | - |
| F92084 | 0.338 | 0.798 | M, A, L, P | - | - | - | - | - | - |
| F100698 | 5.644 | 0.001 | A, P, M, L | ns | 0.026 | 0.009 | ns | ns | ns |
| Forensic 1-2-81 | 3.649 | 0.015 | P, M, A, L | ns | ns | ns | ns | ns | ns |

A = Anterior, P = Posterior, M = Medial, L = Lateral
Post-hoc analyses were only performed if the results of the repeated measures ANOVA proved significant.

## Table 15. Within-Slide Comparison of Osteon Population Density Using Interior Cortex Only with Raw Data

| | *Repeated Measures ANOVA* | | | *Post-hoc Pairwise Comparisons* | | | | | |
|---|---|---|---|---|---|---|---|---|---|
| **Slide ID** | **F** | **p** | **Descending Magnitude** | **A x P** | **A x M** | **A x L** | **P x M** | **P x L** | **M x L** |
| 10995 | 1.570 | 0.271 | M/L, A, P | - | - | - | - | - | - |
| 92297 | 1.673 | 0.249 | A, L, M, P | - | - | - | - | - | - |
| F011398 | 2.220 | 0.163 | L, M, A, P | - | - | - | - | - | - |
| F011691 | 0.664 | 0.597 | A, P/M, L | - | - | - | - | - | - |
| F032798 | 0.196 | 0.896 | L, A, M, P | - | - | - | - | - | - |
| F041700 | 6.972 | 0.013 | A, M, L, P | ns | ns | ns | 0.048 | ns | ns |
| F072098 | 10.833 | 0.003 | A, M, L, P | ns | ns | ns | ns | ns | ns |
| F92084 | 6.658 | 0.014 | L, A, M, P | ns | ns | ns | ns | 0.034 | ns |
| F100698 | 2.293 | 0.155 | M, A, L, P | - | - | - | - | - | - |
| Forensic 1-2-81 | 2.275 | 0.157 | A, M, P, L | - | - | - | - | - | - |

A = Anterior, P = Posterior, M = Medial, L = Lateral
Post-hoc analyses were only performed if the results of the repeated measures ANOVA proved significant.

## Table 16. Within-Slide Comparison of Percent Remodeled Area Using Interior Cortex Only with Raw Data

| | *Repeated Measures ANOVA* | | | *Post-hoc Pairwise Comparisons* | | | | | |
|---|---|---|---|---|---|---|---|---|---|
| **Slide ID** | **F** | **p** | **Descending Magnitude** | **A x P** | **A x M** | **A x L** | **P x M** | **P x L** | **M x L** |
| 10995 | 2.793 | 0.109 | A, M, P, L | - | - | - | - | - | - |
| 92297 | 2.135 | 0.174 | A, L, P, M | - | - | - | - | - | - |
| F011398 | 1.913 | 0.206 | L, M, A, P | - | - | - | - | - | - |
| F011691 | 1.398 | 0.312 | A, P, M, L | - | - | - | - | - | - |
| F032798 | 15.577 | 0.001 | A, P, L, M | 0.003 | 0.038 | ns | ns | ns | ns |
| F041700 | 11.685 | 0.003 | A, M, P, L | ns | ns | 0.001 | ns | ns | ns |
| F072098 | 0.340 | 0.797 | P, M, A, L | - | - | - | - | - | - |
| F92084 | 1.189 | 0.373 | L, M, A, P | - | - | - | - | - | - |
| F100698 | 12.820 | 0.002 | M, A, L, P | ns | ns | ns | 0.012 | ns | 0.047 |
| Forensic 1-2-81 | 1.322 | 0.333 | A, M, P, L | - | - | - | - | - | - |

A = Anterior, P = Posterior, M = Medial, L = Lateral
Post-hoc analyses were only performed if the results of the repeated measures ANOVA proved significant.

## Table 17. Within-Slide Comparison of Osteon Area Using Interior Cortex Only with Rank-Transformed Data

| | *Repeated Measures ANOVA* | | | *Post-hoc Pairwise Comparisons* | | | | | |
|---|---|---|---|---|---|---|---|---|---|
| **Slide ID** | **F** | **p** | **Descending Magnitude** | **A x P** | **A x M** | **A x L** | **P x M** | **P x L** | **M x L** |
| 10995 | 3.608 | 0.017 | A, P, M, L | ns | ns | 0.003 | ns | ns | ns |
| 92297 | 2.046 | 0.115 | P, A, L, M | - | - | - | - | - | - |
| F011398 | 1.704 | 0.174 | P, M, A, L | - | - | - | - | - | - |
| F011691 | 1.070 | 0.367 | P, L, A, M | - | - | - | - | - | - |
| F032798 | 13.935 | <0.001 | A, P, L, M | ns | <0.001 | ns | <0.001 | ns | <0.001 |
| F041700 | 2.578 | 0.060 | P, A, M, L | - | - | - | - | - | - |
| F072098 | 9.863 | <0.001 | P, M, L, A | <0.001 | 0.034 | ns | ns | 0.012 | ns |
| F92084 | 1.224 | 0.304 | L, M, P, A | - | - | - | - | - | - |
| F100698 | 2.071 | 0.110 | A, M, P, L | - | - | - | - | - | - |
| Forensic 1-2-81 | 0.907 | 0.440 | P, L, M, A | - | - | - | - | - | - |

A = Anterior, P = Posterior, M = Medial, L = Lateral
Post-hoc analyses were only performed if the results of the repeated measures ANOVA proved significant.

## Table 18. Within-Slide Comparison of Haversian Canal Area Using Interior Cortex Only with Rank-Transformed Data

| | *Repeated Measures ANOVA* | | | *Post-hoc Pairwise Comparisons* | | | | | |
|---|---|---|---|---|---|---|---|---|---|
| **Slide ID** | **F** | **p** | **Descending Magnitude** | **A x P** | **A x M** | **A x L** | **P x M** | **P x L** | **M x L** |
| 10995 | 8.897 | <0.001 | A, M, P, L | ns | ns | <0.001 | ns | ns | 0.001 |
| 92297 | 2.674 | 0.054 | P, A, M, L | - | - | - | - | - | - |
| F011398 | 6.200 | 0.001 | P, A, M, L | ns | ns | 0.020 | ns | 0.009 | ns |
| F011691 | 1.372 | 0.257 | P, A, L, M | - | - | - | - | - | - |
| F032798 | 0.692 | 0.559 | A, L, P, M | - | - | - | - | - | - |
| F041700 | 8.402 | <0.001 | A, P, M, L | ns | 0.017 | <0.001 | ns | 0.026 | ns |
| F072098 | 1.262 | 0.295 | M, L, P, A | - | - | - | - | - | - |
| F92084 | 1.375 | 0.254 | M, A, P, L | - | - | - | - | - | - |
| F100698 | 5.745 | 0.001 | A, L, P, M | ns | 0.002 | <0.001 | ns | ns | ns |
| Forensic 1-2-81 | 1.363 | 0.258 | P, M, A, L | - | - | - | - | - | - |

A = Anterior, P = Posterior, M = Medial, L = Lateral
Post-hoc analyses were only performed if the results of the repeated measures ANOVA proved significant.

## Table 19. Within-Slide Comparison of Osteon Population Density Using Interior Cortex Only with Ranked-Transformed Data

| | *Repeated Measures ANOVA* | | | *Post-hoc Pairwise Comparisons* | | | | | |
|---|---|---|---|---|---|---|---|---|---|
| **Slide ID** | **F** | **p** | **Descending Magnitude** | **A x P** | **A x M** | **A x L** | **P x M** | **P x L** | **M x L** |
| 10995 | 1.639 | 0.256 | M/L, A, P | - | - | - | - | - | - |
| 92297 | 1.085 | 0.409 | A, L, M, P | - | - | - | - | - | - |
| F011398 | 3.670 | 0.063 | L, M, A, P | - | - | - | - | - | - |
| F011691 | 0.379 | 0.771 | A, M, P, L | - | - | - | - | - | - |
| F032798 | 0.206 | 0.889 | A, L, M, P | - | - | - | - | - | - |
| F041700 | 9.576 | 0.005 | A, M, L, P | 0.008 | ns | ns | ns | ns | ns |
| F072098 | 8.333 | 0.008 | A, M, L, P | 0.031 | ns | ns | ns | ns | ns |
| F92084 | 6.590 | 0.015 | L, A, M, P | ns | ns | ns | ns | ns | ns |
| F100698 | 2.144 | 0.173 | A/M, L, P | - | - | - | - | - | - |
| Forensic 1-2-81 | 1.704 | 0.243 | A, M, P, L | - | - | - | - | - | - |

A = Anterior, P = Posterior, M = Medial, L = Lateral
Post-hoc analyses were only performed if the results of the repeated measures ANOVA proved significant.

## Table 20. Within-Slide Comparison of Percent Remodeled Area Using Interior Cortex Only with Rank-Transformed Data

| | *Repeated Measures ANOVA* | | | *Post-hoc Pairwise Comparisons* | | | | | |
|---|---|---|---|---|---|---|---|---|---|
| **Slide ID** | **F** | **p** | **Descending Magnitude** | **A x P** | **A x M** | **A x L** | **P x M** | **P x L** | **M x L** |
| 10995 | 4.143 | 0.048 | A, M, P, L | ns | ns | ns | ns | ns | ns |
| 92297 | 3.484 | 0.070 | A, L, M, P | - | - | - | - | - | - |
| F011398 | 2.781 | 0.110 | L, M, A/P | - | - | - | - | - | - |
| F011691 | 1.362 | 0.322 | A, P, M, L | - | - | - | - | - | - |
| F032798 | 13.222 | 0.002 | A, P, L, M | ns | 0.007 | ns | ns | ns | ns |
| F041700 | 10.333 | 0.004 | A, M, P, L | ns | ns | 0.034 | ns | ns | ns |
| F072098 | 0.237 | 0.868 | P, M, A, L | - | - | - | - | - | - |
| F92084 | 1.198 | 0.371 | L, M, A, P | - | - | - | - | - | - |
| F100698 | 9.768 | 0.005 | M, A, L, P | ns | ns | ns | 0.017 | ns | ns |
| Forensic 1-2-81 | 2.022 | 0.189 | A, P, M, L | - | - | - | - | - | - |

A = Anterior, P = Posterior, M = Medial, L = Lateral
Post-hoc analyses were only performed if the results of the repeated measures ANOVA proved significant.

**Table 21. Comparison of Remodeling Variables Between 40x and 100x Magnification**

| | Raw Data | | Rank-transformed Data | |
|---|---|---|---|---|
| | t | p | t | p |
| Osteon Area | 0.491 | 0.635 | 0.795 | 0.447 |
| Haversian Canal Area | 0.037 | 0.971 | -0.091 | 0.929 |
| OPD | -4.100 | 0.003 | -3.597 | 0.006 |
| Percent Remodeled Area | -1.560 | 0.153 | -1.365 | 0.205 |

**Table 22. Correlations Between Remodeling Variables and Age Using the Entire Endosteal to Periosteal Column of Cortex**

| | Anterior | | Posterior | | Medial | | Lateral | |
|---|---|---|---|---|---|---|---|---|
| | $r_s$ | p | $r_s$ | p | $r_s$ | p | $r_s$ | p |
| **Osteon Size** | -0.006 | 0.987 | -0.111 | 0.761 | 0.308 | 0.387 | 0.363 | 0.302 |
| **Haversian Canal Size** | 0.554 | 0.097 | -0.203 | 0.574 | 0.579 | 0.080 | 0.572 | 0.084 |
| **OPD** | 0.172 | 0.634 | -0.062 | 0.866 | 0.092 | 0.800 | -0.234 | 0.515 |
| **Percent Remodeled Bone** | 0.092 | 0.800 | 0.289 | 0.418 | 0.363 | 0.302 | -0.043 | 0.906 |

**Table 23. Correlations Between Remodeling Variables and Age Using Interior Cortex Only**

| | Anterior | | Posterior | | Medial | | Lateral | |
|---|---|---|---|---|---|---|---|---|
| | $r_s$ | p | $r_s$ | p | $r_s$ | p | $r_s$ | p |
| **Osteon Size** | -0.252 | 0.482 | -0.086 | 0.813 | 0.222 | 0.538 | 0.160 | 0.659 |
| **Haversian Canal Size** | 0.517 | 0.126 | 0.037 | 0.919 | 0.437 | 0.207 | 0.406 | 0.244 |
| **OPD** | 0.295 | 0.407 | -0.151 | 0.677 | 0.268 | 0.454 | -0.018 | 0.960 |
| **Percent Remodeled Bone** | 0.049 | 0.893 | 0.031 | 0.933 | 0.609 | 0.061 | 0.135 | 0.709 |